Naval Command,
Control and Ocean
Surveillance Center RDT&E Division San Diego, CA
92152-5001

Technical Document 2393
November 1992

A Review of the Ionospheric Model for the Long Wave Prediction Capability

J. A. Ferguson

Technical Document 2393
November 1992

A Review of the Ionospheric Model for the Long Wave Prediction Capability

J. A. Ferguson

NAVAL COMMAND, CONTROL AND OCEAN SURVEILLANCE CENTER
RDT&E DIVISION
San Diego, California 92152-5001

J. D. FONTANA, CAPT, USN
Commanding Officer

R. T. SHEARER
Executive Director

ADMINISTRATIVE INFORMATION

The work for this report was performed by the Ionospheric Branch (Code 542) in the Ocean and Atmospheric Sciences Division (Code 54) of the Naval Command, Control and Ocean Surveillance Center, RDT&E Division. The report covers work performed during the period of FY 92 that was funded by the Space and Naval Warfare Systems Command (PMW-152), Washington, DC.

Released by
Dr. J. A. Ferguson, Head
Ionospheric Branch

Under authority of
Dr. J. H. Richter, Head
Ocean and Atmospheric
Sciences Division

RV

EXECUTIVE SUMMARY

OBJECTIVE

Evaluate the ionospheric model used in the Long Wavelength Propagation Capability (LWPC) using baseline data. Evaluate ionospheric model suggested by the analysis of measurements made aboard the merchant ship *Callaghan*.

RESULTS

1. Baseline data were identified and compared to calculations using the current built-in model of the ionosphere found in the LWPC. The comparisons show that the calculations using the LWPC fit the baseline data generally to within 3 decibels for daytime conditions and to within 6 decibels under nighttime conditions.

2. Baseline data were compared to calculations using the ionospheric model suggested by an analysis of the measurements made aboard the merchant ship *Callaghan*. The new model provides better agreement with the baseline data than the LWPC at night for distances less than about 2000 km, but it is noticeably poorer at distance greater than 2000 km.

RECOMMENDATIONS

1. Since the principal use of the LWPC is for assessing maximum coverage it is important that it be accurate at long ranges. Since the new model is not as good as the LWPC at long ranges at night, it is recommended that the LWPC retain its current ionospheric model.

2. The frequency dependence found in the LWPC for nighttime propagation cannot be resolved with the existing baseline data set. It is recommended that this dependence be examined when more data are available.

CONTENTS

FIGURES

CONTENTS (continued)

TABLES

INTRODUCTION

Propagation of radio waves in the very low frequency (vlf) regime (10 to 30 kHz) and the lower end of the low frequency (lf) regime (30 to 60 kHz) is modeled using a waveguide defined by the earth's surface and the ionosphere. This waveguide model has been described in a series of documents which describe the initial model and its subsequent development [Gossard *et al.* (1966), Pappert, Gossard and Rothmuller (1967), Sheddy, Gough and Pappert (1968), Sheddy et al. (1968), Pappert, Moler and Shockey (1970), Pappert and Smith (1971), Pappert, Shockey and Moler (1971), Pappert and Shockey (1972, 1974), Morfitt and Shellman (1976), Pappert and Ferguson (1986), Shellman (1986), Ferguson and Snyder (1987), Pappert and Hitney (1988)]. Although the model can use profiles of particle density and collision frequency specified as arbitrary functions of height, in practice, exponential profiles of ionospheric electron conductivity (which is essentially the scaled ratio of electron density to collision frequency) are used with positive ions assumed for charge neutrality [Bickel, Ferguson and Stanley (1970), Morfitt (1977), Ferguson (1980) Ferguson, Morfitt and Hansen (1985), Morfitt, Ferguson and Snyder (1981), Pappert and Hitney (1988)]. Exponential profiles are characterized by a slope β, in km^{-1}, and a reference height h', in km. For daytime conditions, typical values of β are 0.2 to 0.5 km^{-1}, and values of h' are 70 to 75 km. Under nighttime conditions, the typical ranges for β and h' are 0.3 to 1.0 km^{-1} and 80 to 90 km, respectively.

BACKGROUND

In the past, we have found data collected aboard in-flight aircraft to be most useful for selecting ionospheric profiles. These data reveal a characteristic pattern of signal interference minima and maxima with distance from the transmitter that provide clues to guide the choice of profile. There is an underlying assumption in this sort of analysis that the ionosphere remains static during the data acquisition period. Due to the high cost of operating aircraft, it is unusual to find more than one pass over the same path. Furthermore, the profiles so determined represent only a snapshot of the environment. Consequently, previous selection of ionospheric profiles that produce calculations which agree with measurements has been a hit or miss affair, depending on the sophistication of the propagation model, the complexity of the path over which data were taken and the amount of computer time available.

PURPOSE OF REPORT

The purpose of this report is to examine the fit between calculations using two different models of the ionosphere and a set of what we will call baseline measurements. The first model of the ionosphere is found in the current LWPC (Ferguson & Snyder, 1989a,

1989b). The parameters of that model were manually selected by reviewing the analyses presented by Morfitt (1977) and Ferguson (1980). A systematic review of the ionospheric model in the LWPC, as it pertains to the baseline data, is presented in this report. More recently, a large volume of data were collected aboard a merchant ship named the *Callaghan*. While the baseline data were collected all over the world and over a long span of time, the *Callaghan* data are restricted to the North Atlantic Ocean and a period of one year. These data lend themselves to a systematic analysis for determining the best fit ionospheric model, that has been completed and described elsewhere (Ferguson, 1992). This analysis suggests a modification of the ionospheric model used in the LWPC. This report presents a systematic comparison of the baseline data with the model suggested by the *Callaghan* data. It is important to note that this analysis serves two purposes: evaluation of the exiting LWPC and improvement of the model to be used in the LWPC.

BASELINE MEASUREMENTS AND REPORTED BEST FIT PROFILES

The data used to define the ionospheric profiles used in the LWPC were taken primarily from Morfitt (1977) and Ferguson (1980). These data represent a large number of samples under daytime and nighttime conditions. The data are classified as daytime or nighttime depending on whether the data were collected when the whole propagation path was all day or night. This report presents a systematic examination of the range of conditions which apply to the data. Appendix A contains a summary listing of the data found in the two sources cited. There are 71 daytime cases and 113 nighttime cases. Some of the nighttime cases include both transverse electric (TE) as well as transverse magnetic (TM) data.

The list shows the data in two major groups: day (*D*) and night (*N*). Within each group, the list is arranged in order of frequency (*Freq*), latitude (*Tlat*) and longitude (*Tlon*) of the transmitter, the geographic bearing angle of the measurement path and date of the measurement. The column labeled SSN is the Zurich smoothed sunspot number for the month in which the measurements were made. The columns labeled *Rpt* and *Fig* show the number of the report and the figure in the report from which the data were taken. Report number 141 is Morfitt (1977) and 530 is Ferguson (1980).

In Morfitt (1977) and Ferguson (1980), most of the data were compared to calculations using exponential profiles. We compared the fit between the calculations and the measurements shown in these reports and if the agreement was (subjectively) good, we entered the values of β and h' into the last two columns of the list. This selection is consistent with that used to select the current ionospheric model used in the LWPC. The procedures to be described in this report are an attempt to make such choices objectively.

Plots of β and h' together with the frequency for day and night conditions are shown in figures 1 and 2. These data were taken from Appendix A. The open squares show the

values of frequency with its axis on the left and the filled squares in the top and bottom panels show β and h', respectively, using the axis on the right. The horizontal axis in these plots simply represents a counter for each sample of data from the appendix after sorting by frequency. In the daytime, the values of β range from 0.3 to 0.5 km^{-1}, and h' range from 70 to 75 km. The combination of β equal to 0.5 km^{-1} and h' equal to 70 km occurs only six times in the set of 71 daytime samples. As we shall see later, there is no clear distinction in the conditions under which this combination of β and h' occurs. Under nighttime conditions, the results are much more confusing. The value of β generally increases with frequency, but at frequencies above 30 kHz it takes on a value of 0.7 or 1.2 km^{-1}. At the same time, the values of h' range from 76 to 88 km. The two different values of β above 30 kHz are obtained from only two sets of measurements made on 30 January and 1 February 1974. It is interesting to note that at the higher frequencies, where β oscillates between 0.7 and 1.2 km^{-1}, h' is constant at 88 km. The current LWPC makes h' dependent on magnetic latitude at night which removes some of the ambiguity shown in this figure.

Plots of β and h' *versus* sunspot number for day and night conditions from Appendix A are shown in figures 3 and 4 to take a crude look at the dependence of the profile parameters on solar activity. The first finding we note is that all but 3 samples of the daytime data and two-thirds of the nighttime data were taken when the sunspot numbers were less than 30. There is insufficient data from which to draw any conclusions regarding any dependence of β and h' on solar activity under day or night conditions.

Figure 5 shows the daytime data organized according to solar zenith angle at the midpoint of the propagation path. The baseline data were collected aboard an in-flight aircraft so the solar zenith angle varies along each path. In preparation of this figure, we computed the solar zenith angle at the midpoint of each flight. Since we do not have start and end times for every flight, there are fewer points in this figure than in previous daytime cases. The results shown here are somewhat disconcerting, since we expected some sort of solar zenith angle control. However, most of the data were collected when the solar zenith angle at the midpoint of the path was at about 45°; hence, there is insufficient data to distinguish between β equal to 0.3 and 0.5 km^{-1} based on the solar zenith angle.

Figure 6 shows the nighttime data organized according to the corrected geomagnetic latitude of the path midpoint. Similar to the previous figure, we do not have start and end times for all of the flights so there are fewer points in this figure than in the previous nighttime figures. Paths which are generally north to south should show a marked variation in latitude. However, most of the paths in the baseline data set are almost entirely inside or outside of the polar cap so the midpoint does a good job of sorting out the high latitude data from the middle latitude data. We see that the value of h' tends to be steady near 87 km when the corrected geomagnetic latitude is below 50°; while β varies quite a

bit. On the other hand, at latitudes higher than 50°, h' varies a lot and β is somewhere between 0.3 and 0.6 km^{-1}. We note that h' at the higher latitudes also tends to be lower than at the lower latitudes, consistent with the model and earlier observations.

LWPC PROFILES

We used the LWPC in its current configuration to make calculations for each set of measurements listed in the appendix. Table 1 summarizes the parameters of the ionospheric profile in the LWPC. Note that the application of this model requires the values of β be interpolated linearly with frequency between the two frequency values for nighttime. All other parameters are held constant for all frequencies.

Table 1. Ionospheric profile in the LWPC.

Frequency	Day		Night	
	β	h'	β	h'
kHz	km^{-1}	km	km^{-1}	km
10	0.3	74	0.3	87
60	0.3	74	0.8	86

CALLAGHAN MEASUREMENTS AND BEST FIT PROFILES

The data from the *Callaghan* measurements were signal strength as a function of distance from the transmitters at Annapolis, MD, radiating at 21.4 and 51.6 kHz, and at Cutler, ME, radiating at 24 kHz; the transmitters in Rugby, England, radiating at 16 kHz, and in Anthorn, England, radiating at 16.4 kHz. Data were recorded aboard the Military Sealift Command ship, *Callaghan*, from 29 March 1985 through 18 April 1986. During this period the ship made 50 crossings of the North Atlantic, each crossing taking about a week. The data recorded during these crossings are unique in the large number of measurements repeated at various distances from the transmitter over a long time, thus permitting examination of the variability of the signal in space and time. The track of the ship varied with the tides and the weather, but a lot of the data were recorded along a corridor from the eastern coast of the United States and from the area around England southwest into the middle of the North Atlantic Ocean. These data were analyzed using a new, computer-aided technique that determined the most frequently occurring profile over a distance range from 0 to 4000 km from each transmitter (Ferguson, 1992).

Figure 7 shows a summary of the values of β and h' obtained from contour analysis with the data for both day and night propagation. In each panel, the solid straight line

represents parameter variations used in the LWPC based on the results suggested by Morfitt (1977) and Ferguson (1981). In the daytime, β shows three of the five values along the dashed line which crosses $\beta = 0.3$ km^{-1} at 10 kHz and 0.26 km^{-1} at 60 kHz. The values at 16 and 19 kHz are below and above this line, respectively. The results for h' are less scattered with four of the five values close to 73.5 km. The variation of β at night show some scatter about the linear fit, but the values of h' are quite close to the linear fit which is not as steep as that used in the LWPC. It is speculated that part of the difference between the parameter variations shown in the solid versus the dashed lines will be found to be in the difference in solar activity during the data collection periods. It should be noted that the daytime parameters shown in figure 7 are not very different from the ones used in the LWPC. Hereafter, this model of the ionosphere will be called the *Callaghan* model. Table 2 summarizes the parameters of this model. As with the LWPC model, we used this model to make calculations for each set of measurements listed in the appendix.

Table 2. *Callaghan* ionospheric profile.

Frequency	Day		Night	
	β	h'	β	h'
kHz	km^{-1}	km	km^{-1}	km
10	0.30	75	0.5	85
60	0.26	73	0.6	84

SAMPLE COMPARISONS

In the following, we present a few comparisons between the current LWPC and the *Callaghan* model. Since the daytime models are very similar, only nighttime cases will be shown. Figure 8 shows comparisons of amplitude measurements and calculations using the two models of the ionosphere. The top pair of curves in each figure are the measurements and the calculations (dashed and solid, respectively) expressed in decibels (dB) above 1μV/m. The difference between the measurements and calculations is shown in the middle dashed curve. The data are for 17.1 kHz along a path from Hawaii to Southern California. The results for the LWPC model are generally in good agreement with the data between 1000 and 3000 km. The *Callaghan* model is in good agreement between 500 and 2500 km. Near 3000 km, the LWPC model predicts signals too low and the *Callaghan* model predicts too high. Figure 9 shows comparisons of measurements and calculations for 21.8 kHz along a path from Hawaii to Southern California. The calculations using the

LWPC model are very close to the measurements between 1000 and 4000 km. Over this same range, the *Callaghan* model does not fit the data as well there being a shift of the calculated minima away from the transmitter. However, between 500 and 1200 km, the agreement between measurements and calculations using the *Callaghan* model is much better than that obtained using the LWPC model.

Figure 10 shows comparisons of measurements and calculations for 52.9 kHz along a path from Hawaii to Southern California. We might expect the *Callaghan* model to be better than the LWPC because the former is based on data recorded very close in frequency to this sample of data. Indeed, we see that the calculations using the *Callaghan* model seem to be in better agreement with the measurements, mostly because the calculated amplitudes are higher than those computed using the LWPC model. Overall, the shape of the calculations using the *Callaghan* model is closer to the measurements especially beyond 2000 km. The best fit to these data required a β of 0.7 km^{-1} which is closer to the value used in the *Callaghan* model than in the LWPC model.

SCATTER PLOTS

The most straightforward way to compare the large number of data sets using these two ionospheric models is to make scatter plots. As a measure of "goodness of fit", the data for these plots were generated by computing the average of the absolute difference between the calculations and measurements over short, 500-km distance intervals. The scatter plots were generated for a series of distance ranges: 500 to 1000; 1000 to 1500; 1500 to 2000; 2000 to 2500; 2500 to 3000; and 3000 to 5000 km. Note that points below the 45° line indicate the *Callaghan* model to be superior; whereas, for those above, the original LWPC model is superior.

Figures 11 through 15 are scatter plots for daytime propagation. As expected, the data points lie predominantly along the 45° line. This shows that the average absolute difference between data and model results is independent of the two available profile models. In the distance range, from 100 to 1500 km, there is the most scatter about the 45° line. This is probably due to small errors in locating the first major minimum in the signal strength versus distance pattern. In the distance range from 1500 to 2000 km, the *Callaghan* model is slightly better than the LWPC model, when both models are 9 to 12 dB different from the measurements.

The LWPC model had a constant β and the *Callaghan* model has a slight variation of β with frequency. We consider only the 10 frequency sounder data in examining the impact of this frequency dependence. In each panel of figure 16, there are three sets of data, one for each measurement of sounder signals. Each set of data in this figure represents the root-mean-square (rms) deviation of the calculations from the measurements in each 500 km distance range from 500 to 8000 km; thus, above each frequency

there is a cluster of bars, one for each distance interval. All of the sounder measurements were made in February of 1974, two sets from the transmitter in Hawaii and one from the transmitter in Sentinel, Arizona. The two sets of data, collected on 2 February, were obtained while the aircraft flew on a path from Hawaii towards the transmitter in Arizona. As we might expect, the results from each model are nearly identical to each other.

Figures 17 through 21 are scatter plots for nighttime propagation. In the close range interval from 500 to 1000 km (figure 17) the *Callaghan* model gives slightly better results than the LWPC model. In the distance ranges 1000 to 1500 km and 2000 to 2500 km (figures 18 and 19) the LWPC model is 3 dB worse than the *Callaghan* model when the errors are greater than 9 dB. In the distance range from 1500 to 2000 km, however, the *Callaghan* model is 3 dB worse when the errors are less than 6 db. In the ranges 2000 to 2500 km and 2500 to 3000 km (figures 20 and 21), the LWPC model fits the data better than the *Callaghan* model, when the errors are less than 6 dB.

The LWPC model has a markedly greater variation of β with frequency than the *Callaghan* model. The variation of β with frequency in the LWPC model was inferred from the measurements of the 10 frequency sounders located in Hawaii and Arizona. There are five sets of these measurements, one in 1969 and four in 1974. A set of plots similar to those in figure 16 are shown in figure 22. The LWPC model shows errors about 2 dB larger than the *Callaghan* model for February, 1969, and January, 1974. The errors, for 1 February 1974, are larger for the *Callaghan* model at the low frequencies and smaller at the higher frequencies. This indicates that the frequency dependence of β is more pronounced on this date. This is confirmed by examination of figure 7. For some unexplained reason, the data from the transmitter in Arizona are sparser than the others; nevertheless, there is little difference between the results of the two ionospheric models. It is clear that the issue of the frequency dependence of β is unresolved and needs more data for analysis.

CONCLUSION

The LWPC and *Callaghan* ionospheric models give calculations that are typically less than 6 dB from the measurements. Under daytime conditions, the calculations are frequently within 3 dB of the measurements. Changing to the ionospheric parameters suggested by the *Callaghan* model will not significantly modify the results of the LWPC. However, the fact that the *Callaghan* model was developed in a systematic manner is in its favor. A limited set of 10 frequency sounder data suggest a different variation of β with frequency than is found from the *Callaghan* data, but the results shown in figure 22 suggest that the trade-off is a uniform error over all sets of measurements versus a good fit to two of three sets of data. More data is required to resolve this problem. Another unresolved problem with these models is the dependence of the ionospheric parameters

on solar activity. This problem is being addressed by an ongoing data collection campaign.

As mentioned in the introduction, there are two purposes for collecting and analyzing more data (over the previously existing aircraft data base). The original aircraft data base is sparse. There are only a few propagation paths which have been sampled more than once and rarely is an ionospheric or geophysical condition reproduced; thus, the shipboard measurements provide us, for the first time, multiple samples of data for similar conditions and paths. The analysis described in this report give us confidence that the daytime assessments obtained from the LWPC are valid and quite accurate. Furthermore, under nighttime conditions, which heretofore have not been routinely used to perform coverage assessments, the LWPC does an adequate job of fitting the data. It is clear that for ranges under 2000 km, the model obtained from the *Callaghan* data provide a significant improvement over the LWPC; however, we must consider that the primary purpose of the LWPC is coverage assessment which usually translates to maximum range for any specific mix of frequency, power, and signal processing. In that context, the existing LWPC model is somewhat better than the *Callaghan* model; consequently, it is recommended that the *Callaghan* model not be implemented in the LWPC.

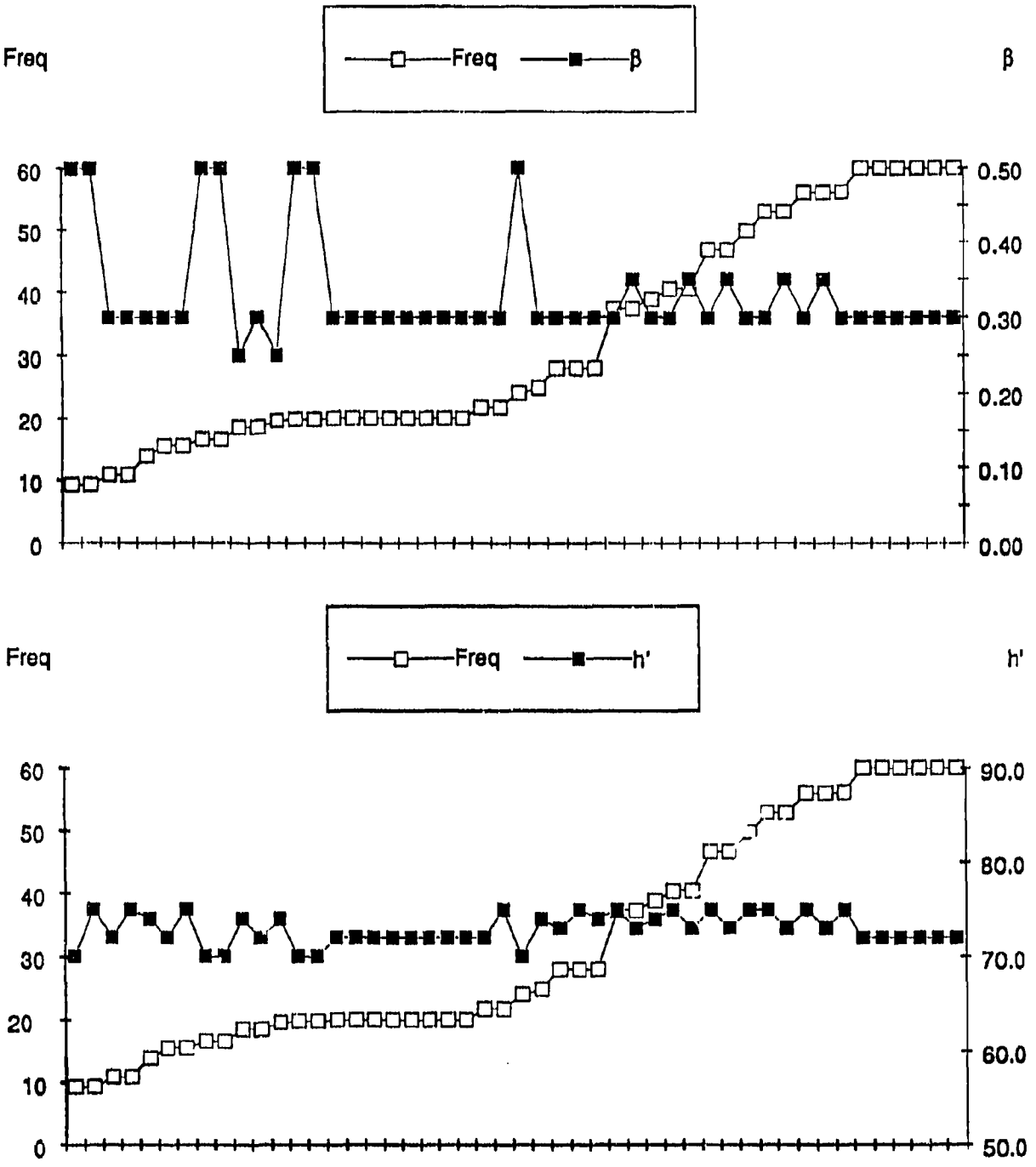

Figure 1. β and h' vs. frequency; day.

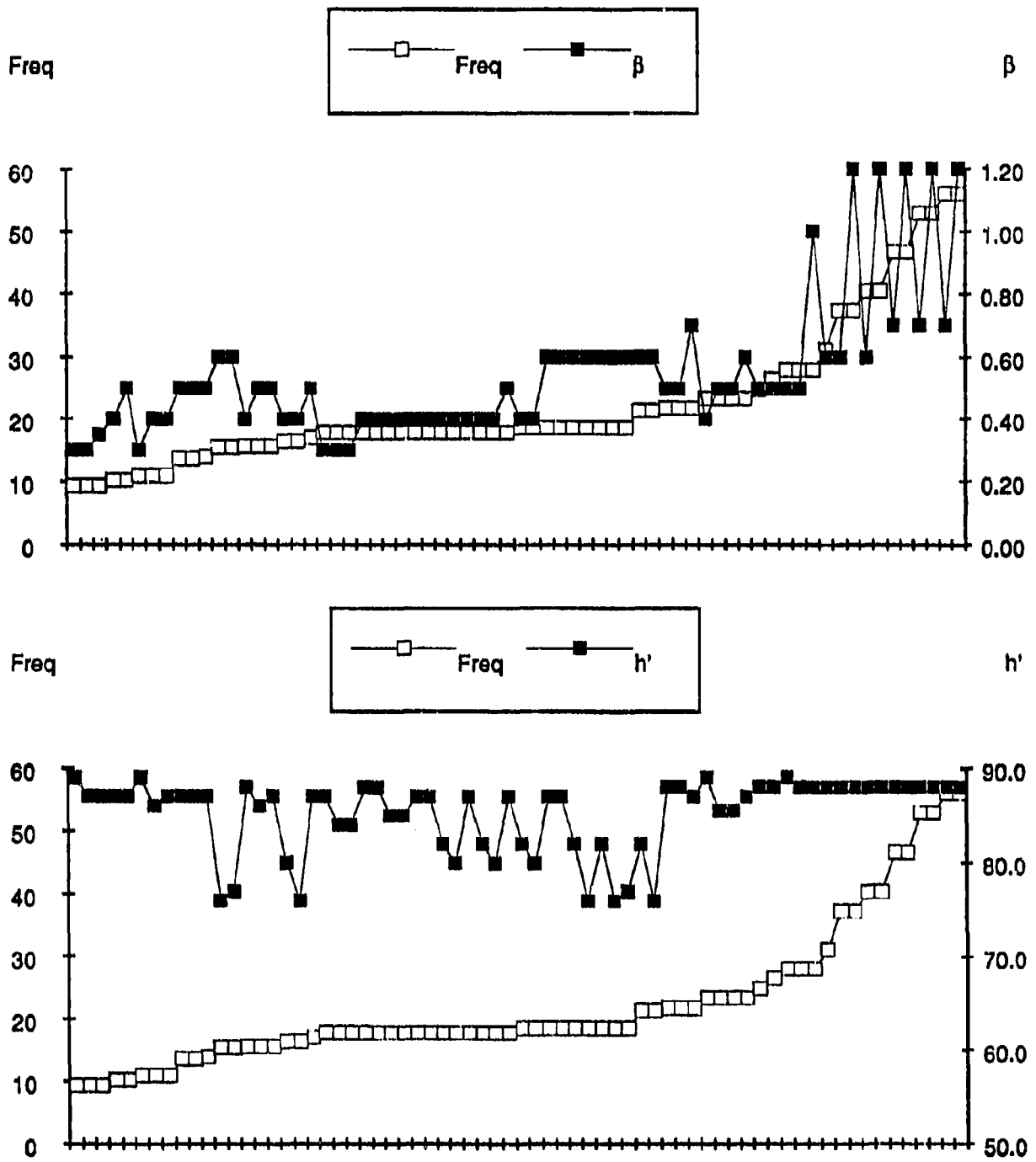

Figure 2. β and h' vs. frequency; night.

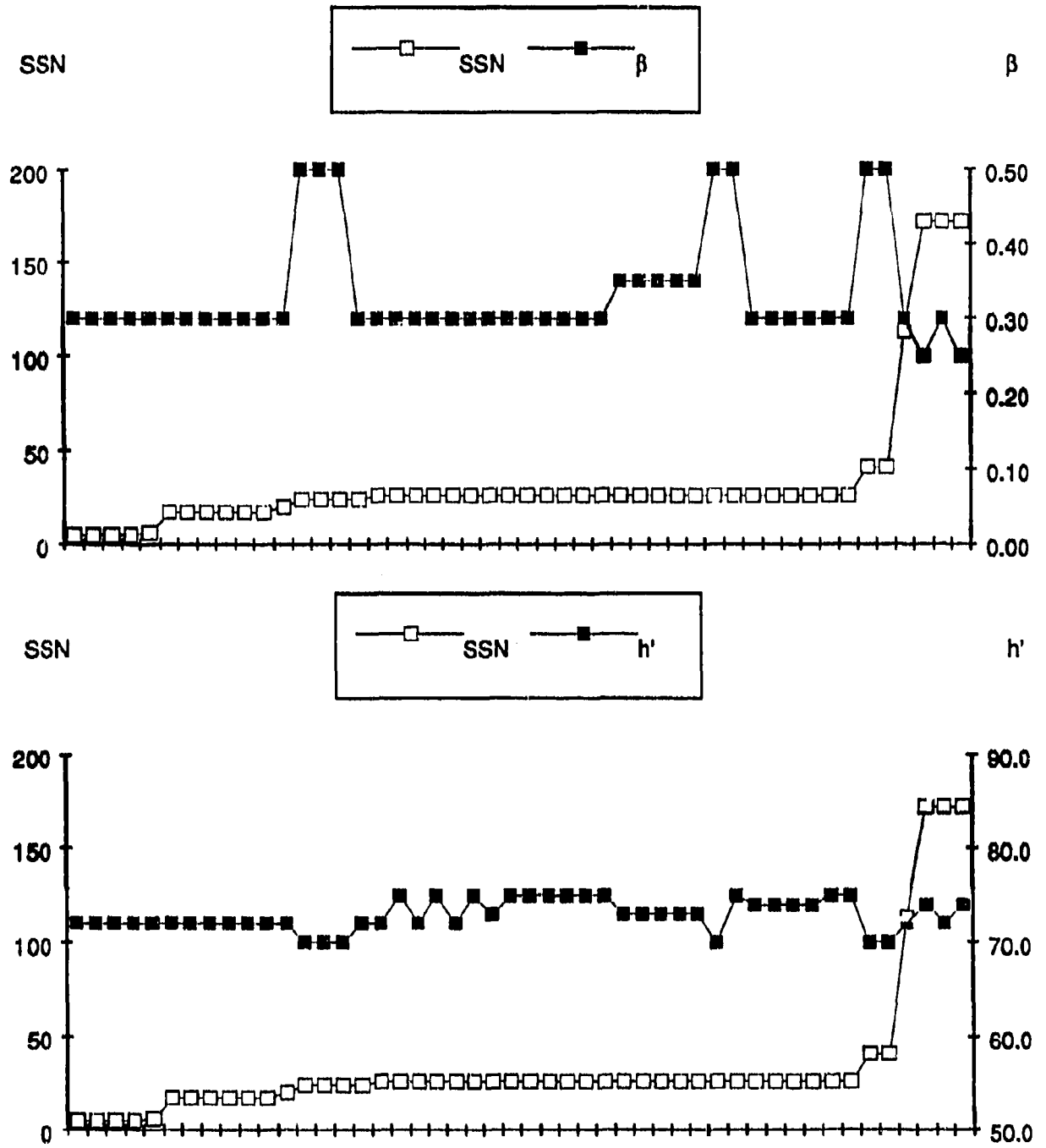

Figure 3. β and h' vs. sunspot number; day.

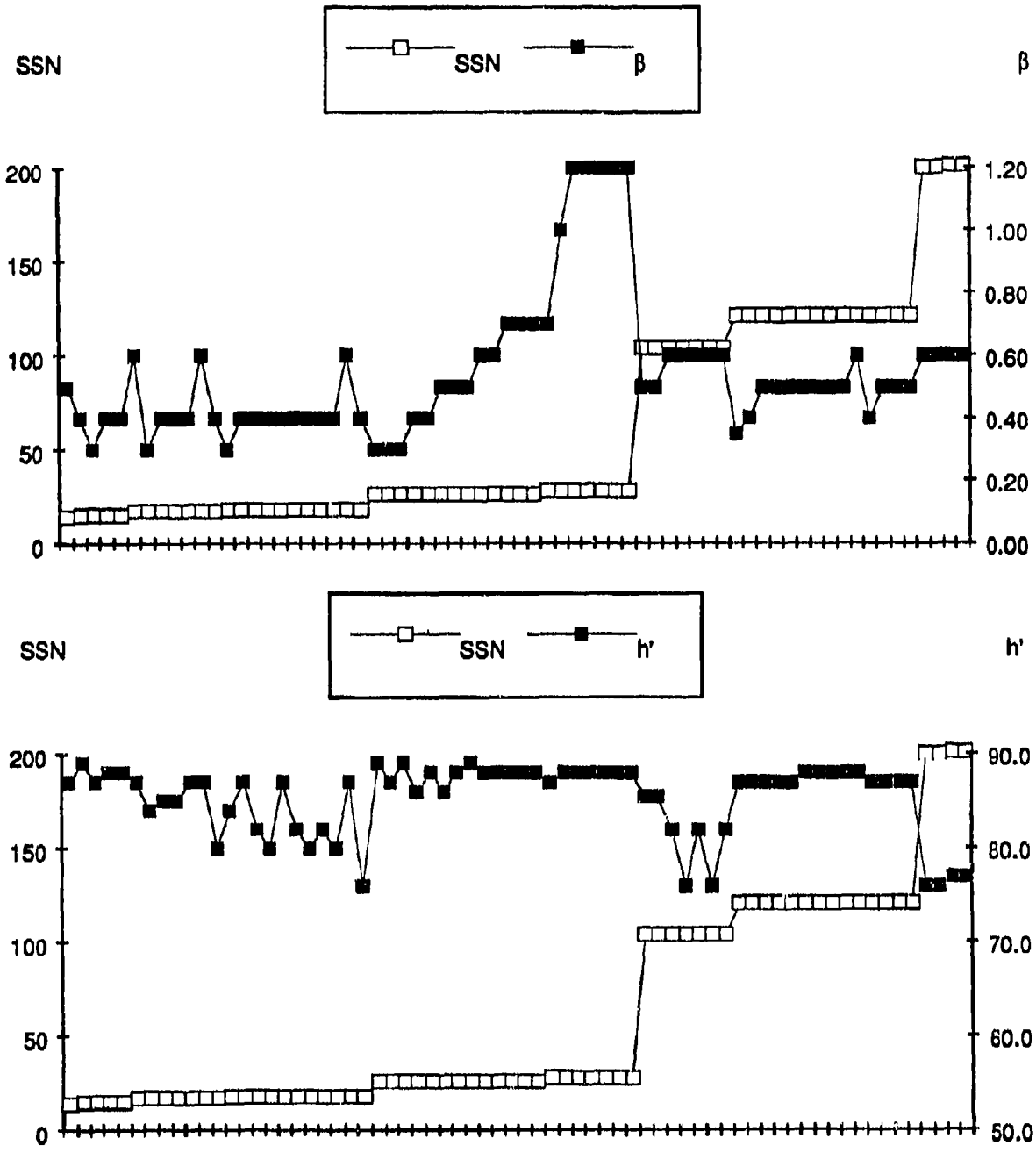

Figure 4. β and h' vs. sunspot number; night.

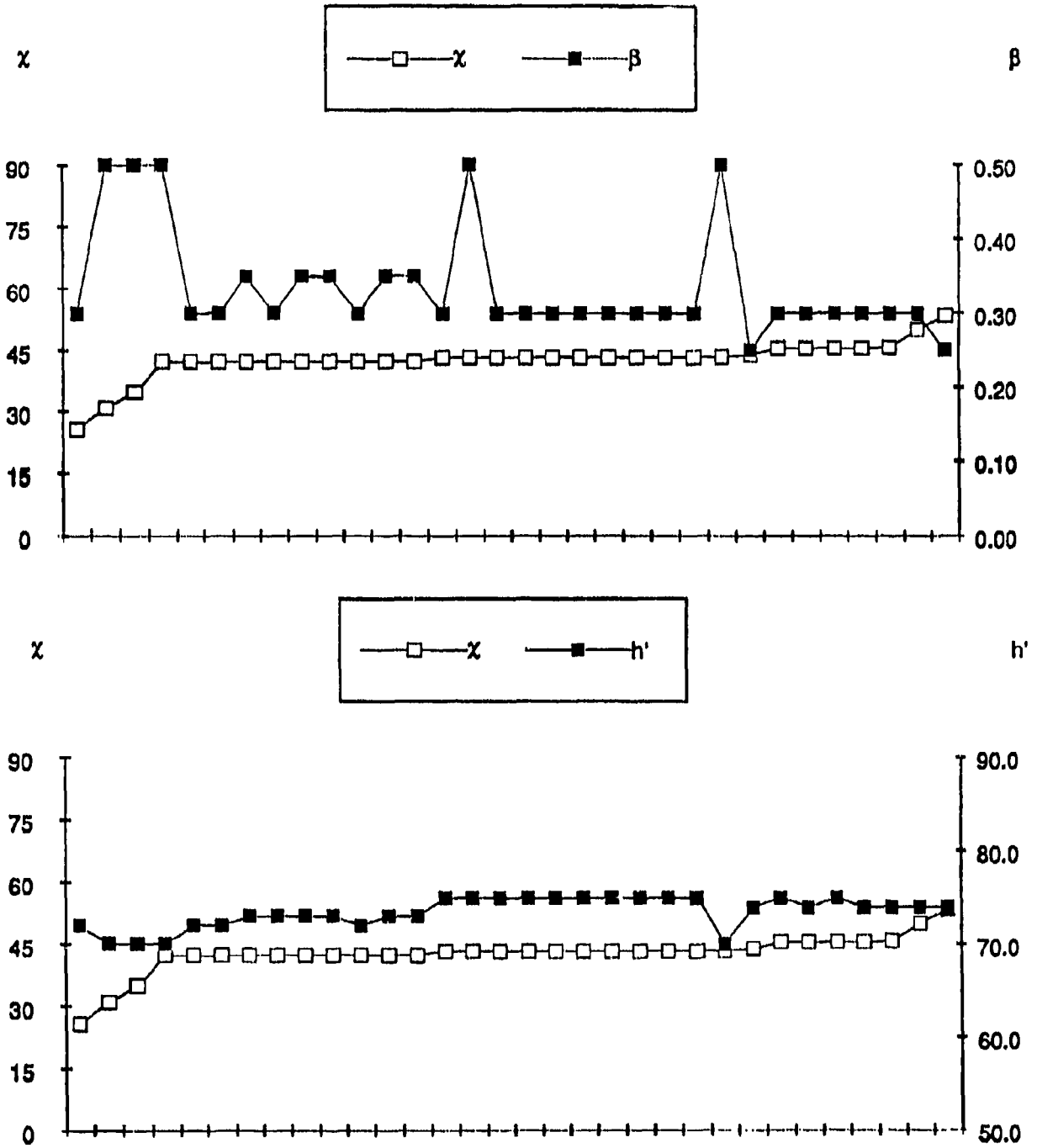

Figure 5. β and h' vs. solar zenith angle; day.

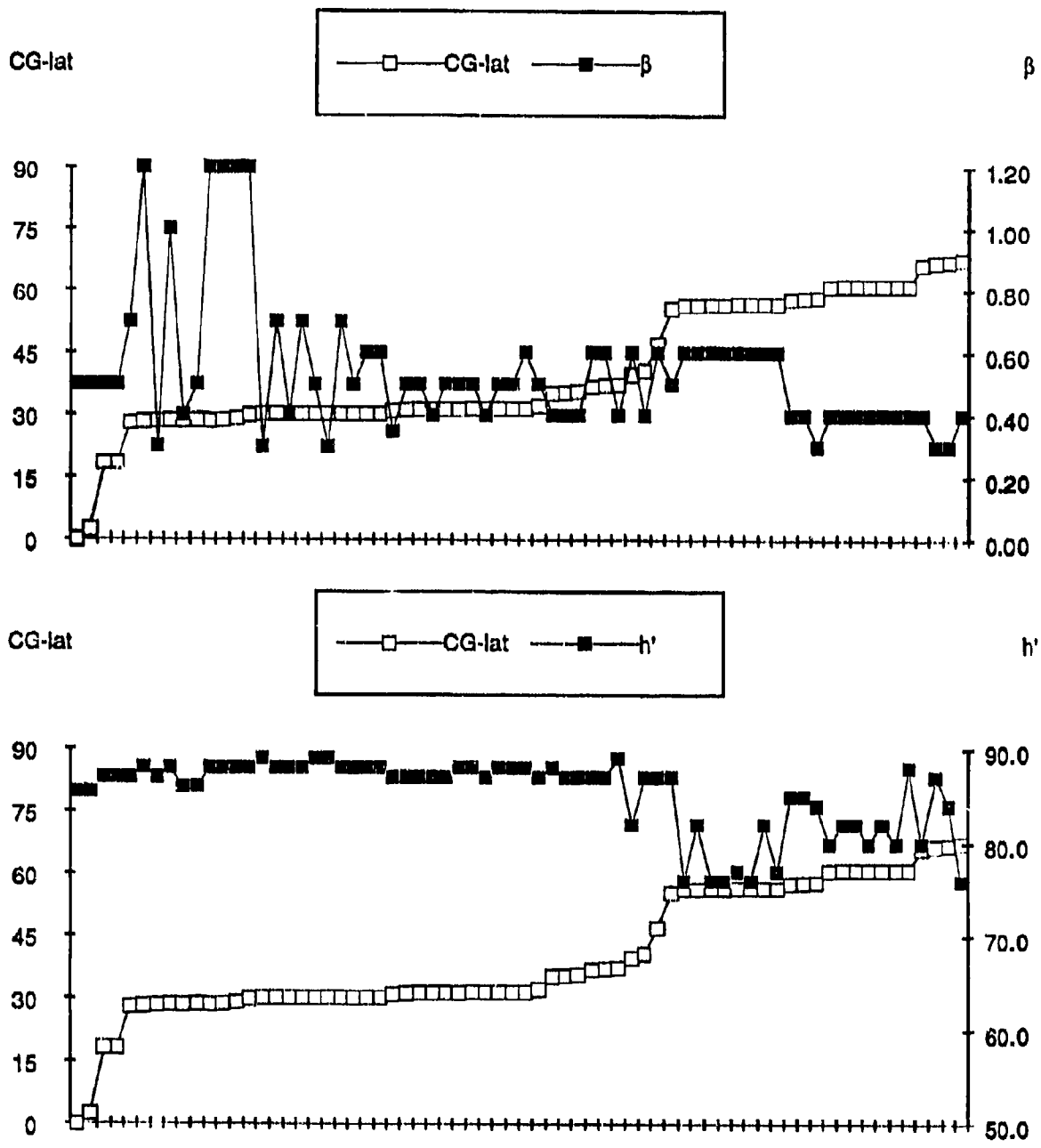

Figure 6. β and h' vs. corrected geomagnetic latitude; night.

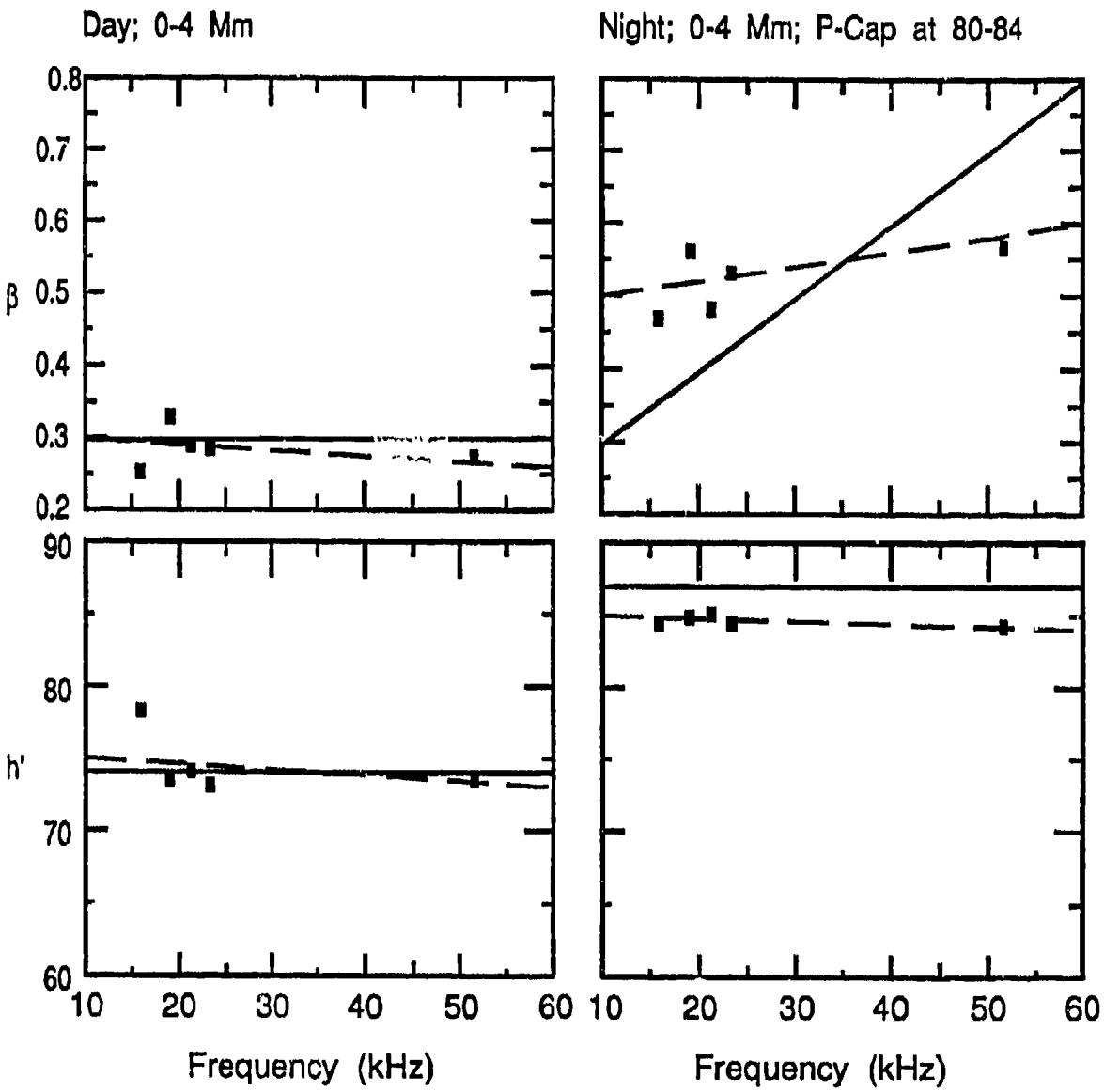

Figure 7. β and h' vs. frequency from contour analysis. The solid line shows the variation used in the LWPC and the dashed line is the best fit to the Callaghan parameters.

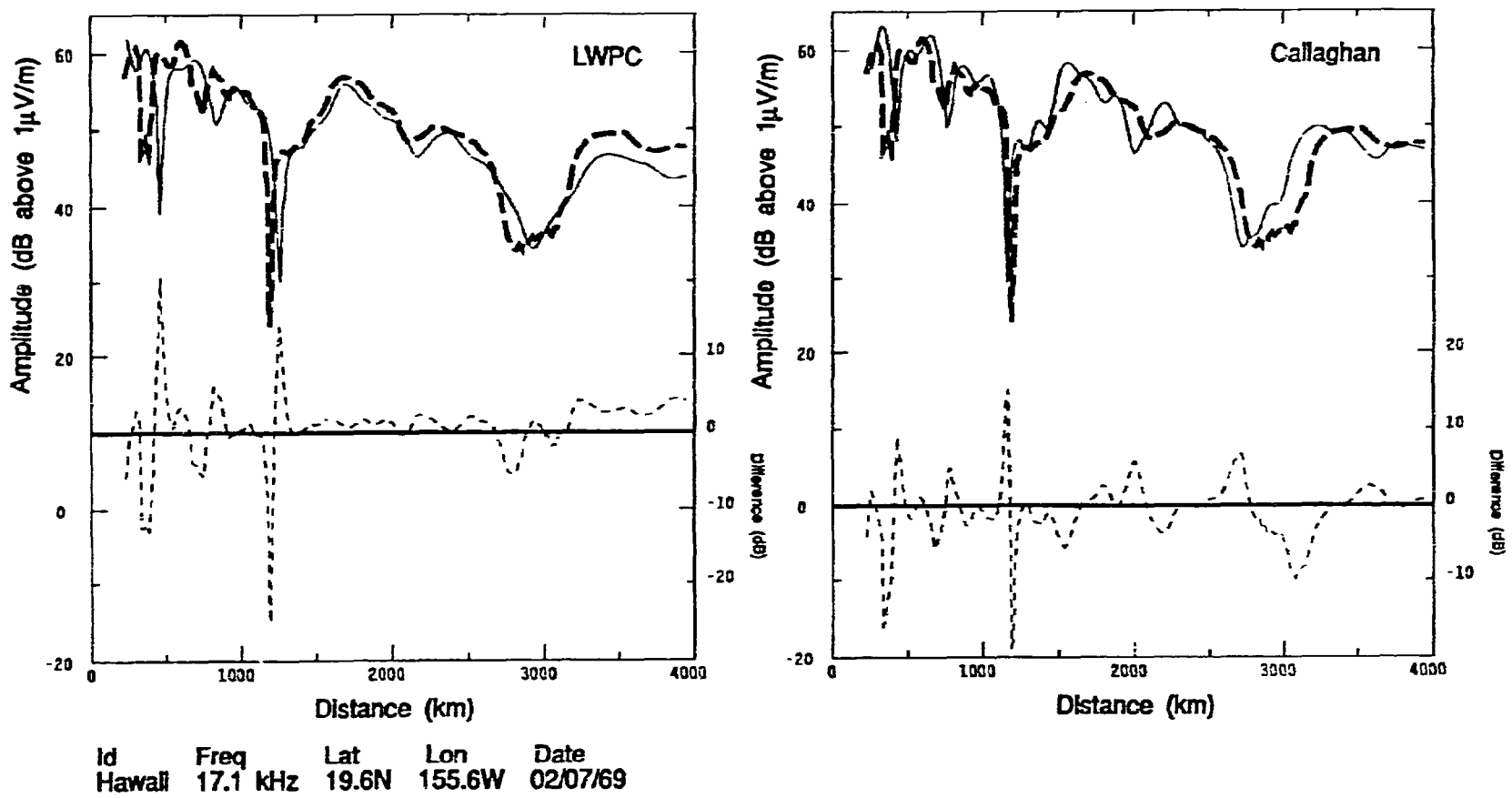

Figure 8. Comparison between measurements and calculations at 17.1 kHz along a path from Hawaii to Southern California under nighttime conditions.

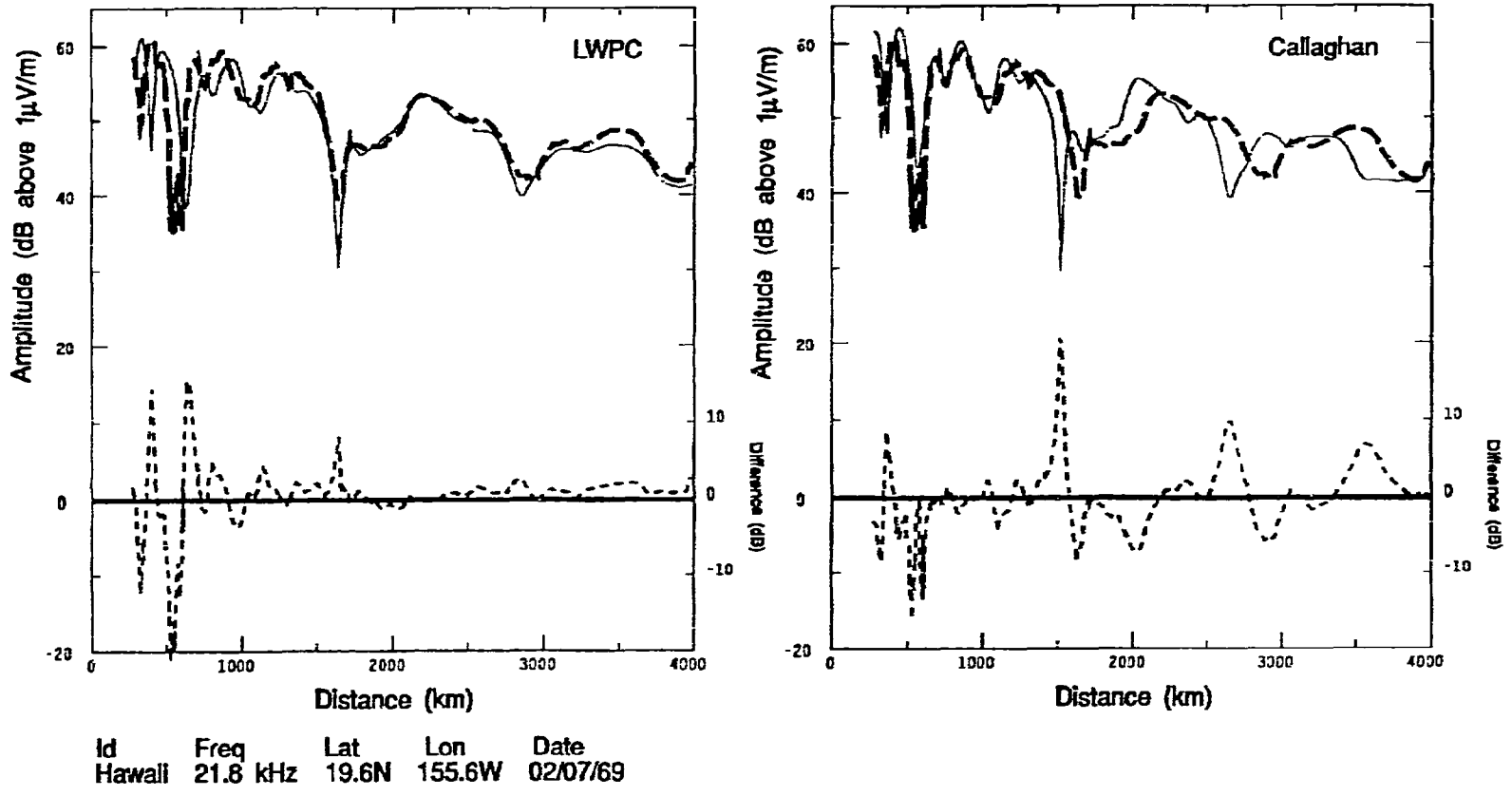

Figure 9. Comparison between measurements and calculations at 21.8 kHz along a path from Hawaii to Southern California under nighttime conditions.

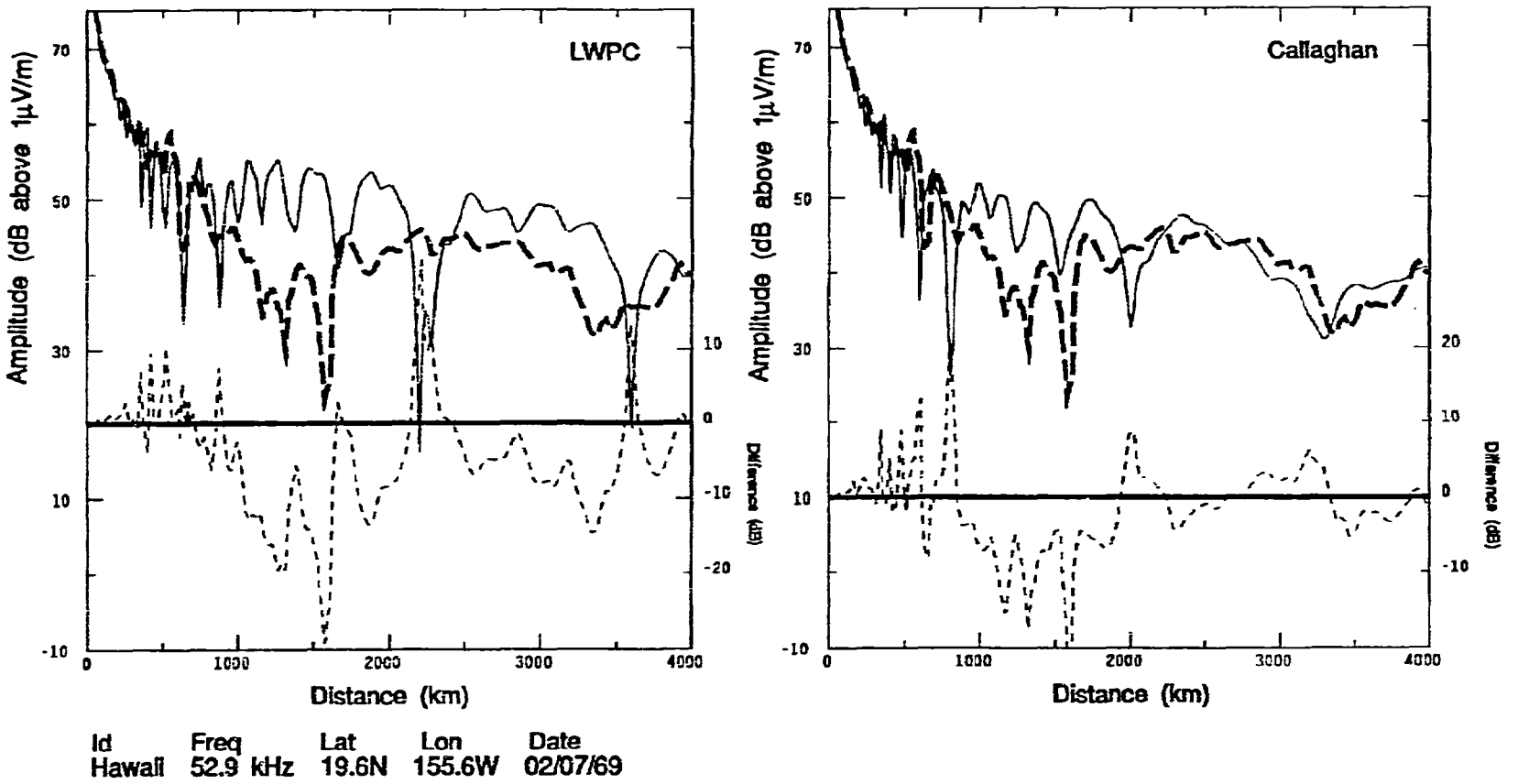

Figure 10. Comparison between measurements and calculations at 52.9 kHz along a path from Hawaii to Southern California under nighttime conditions.

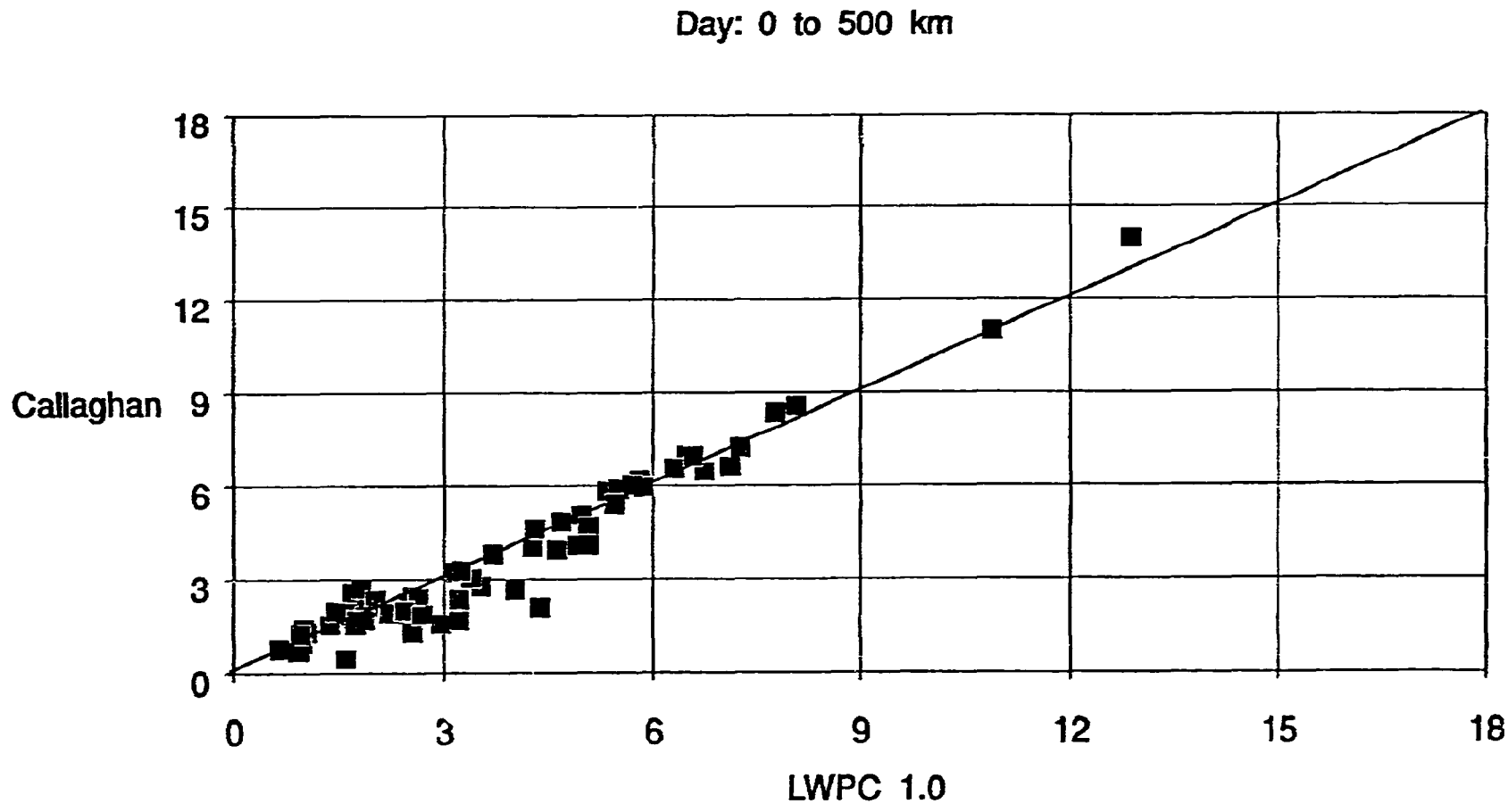

Figure 11. Scatter plot of the average absolute difference between the measurements and calculations using each ionospheric model over the distance range from 500 to 1000 km under daytime conditions.

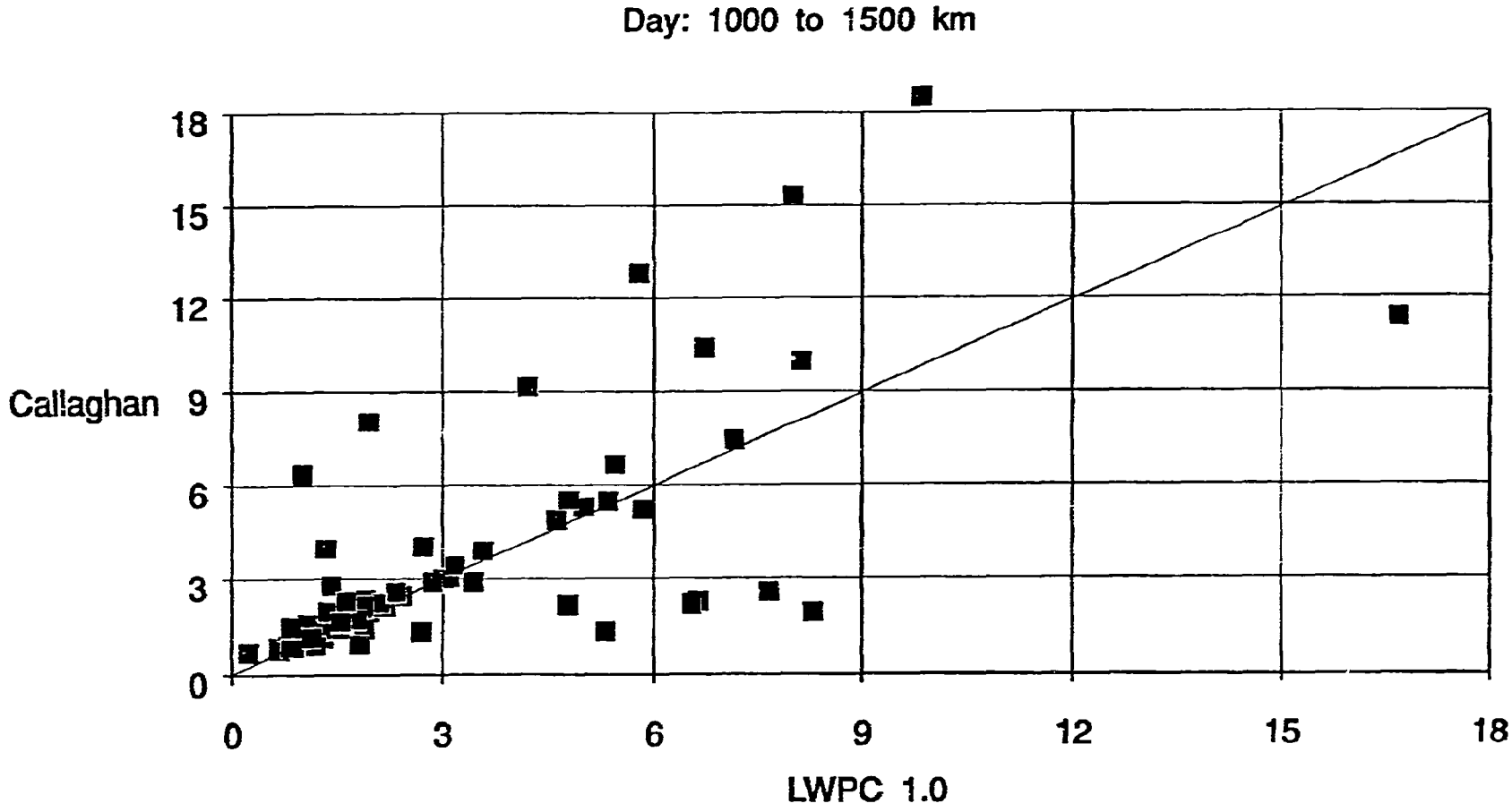

Figure 12. Scatter plots of the average absolute difference between the measurements and calculations using each ionospheric model over the distance range from 1000 to 1500 km under daytime conditions.

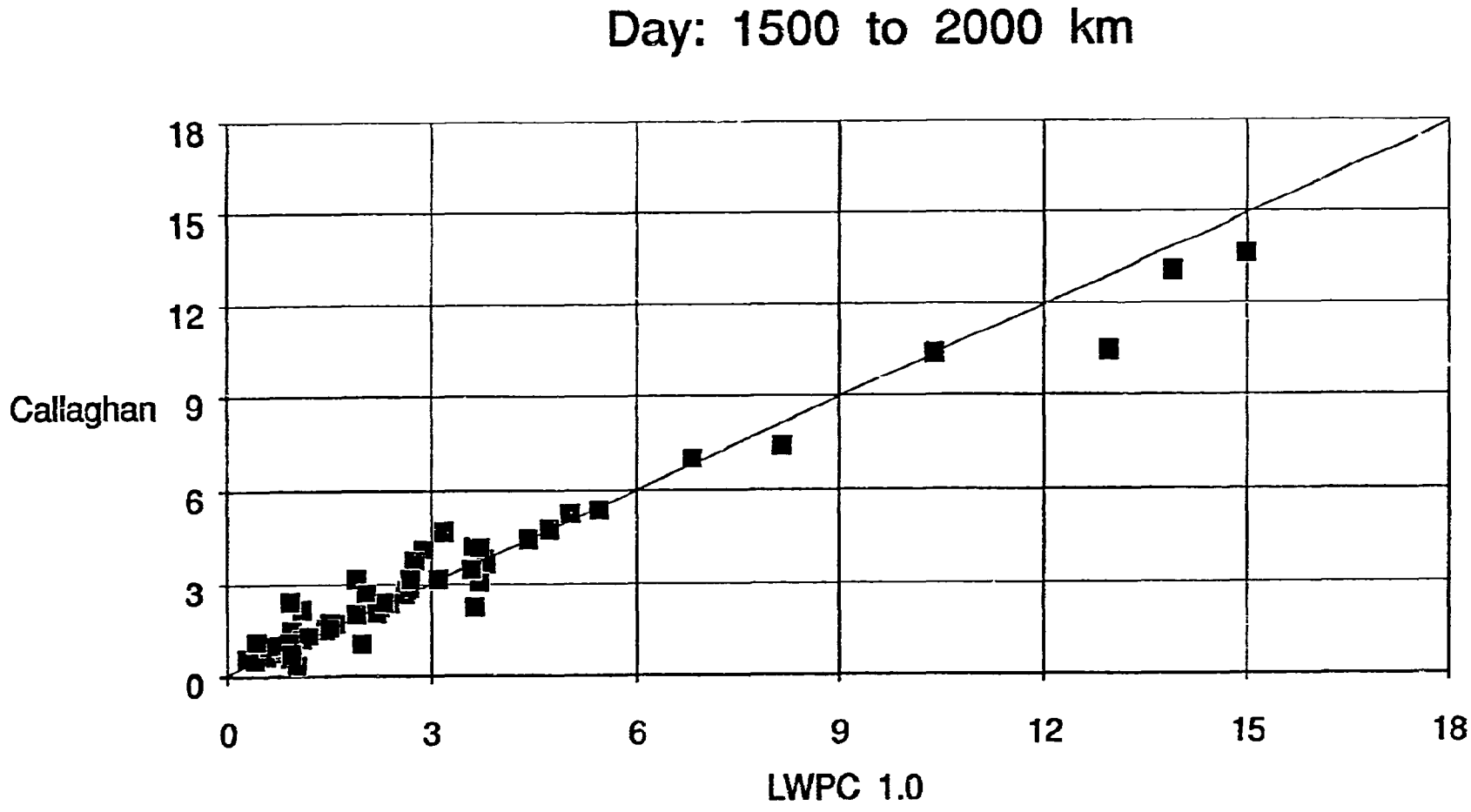

Figure 13. Scatter plot of the average absolute difference between the measurements and calculations using each ionospheric model over the distance range from 1500 to 2000 km under daytime conditions.

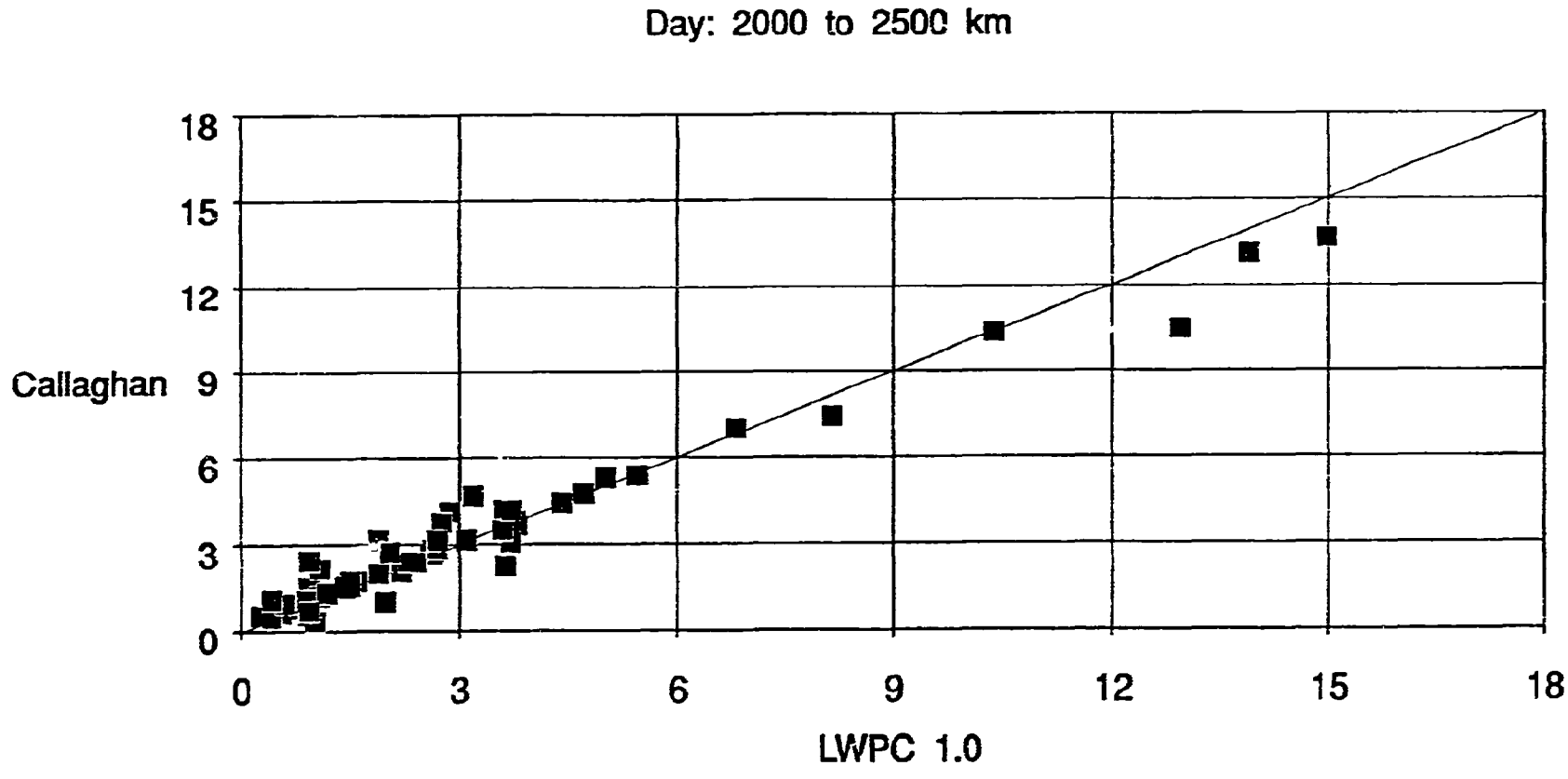

Figure 14. Scatter plot of the average absolute difference between the measurements and calculations using each ionospheric model over the distance range from 2000 to 2500 km under daytime conditions.

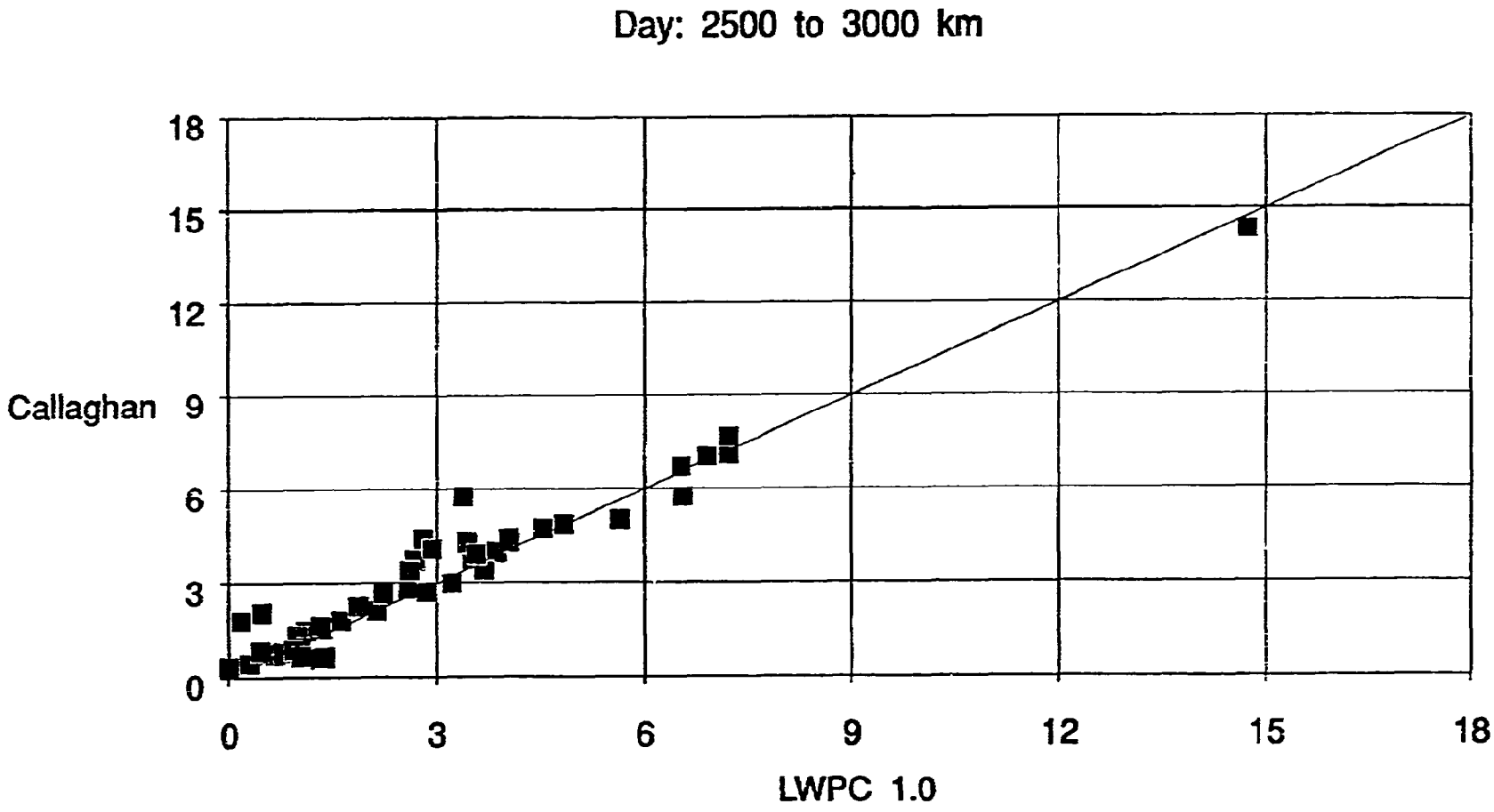

Figure 15. Scatter plot of the average absolute difference between the measurements and calculations using each ionospheric model over the distance range from 2500 to 3000 km under daytime conditions.

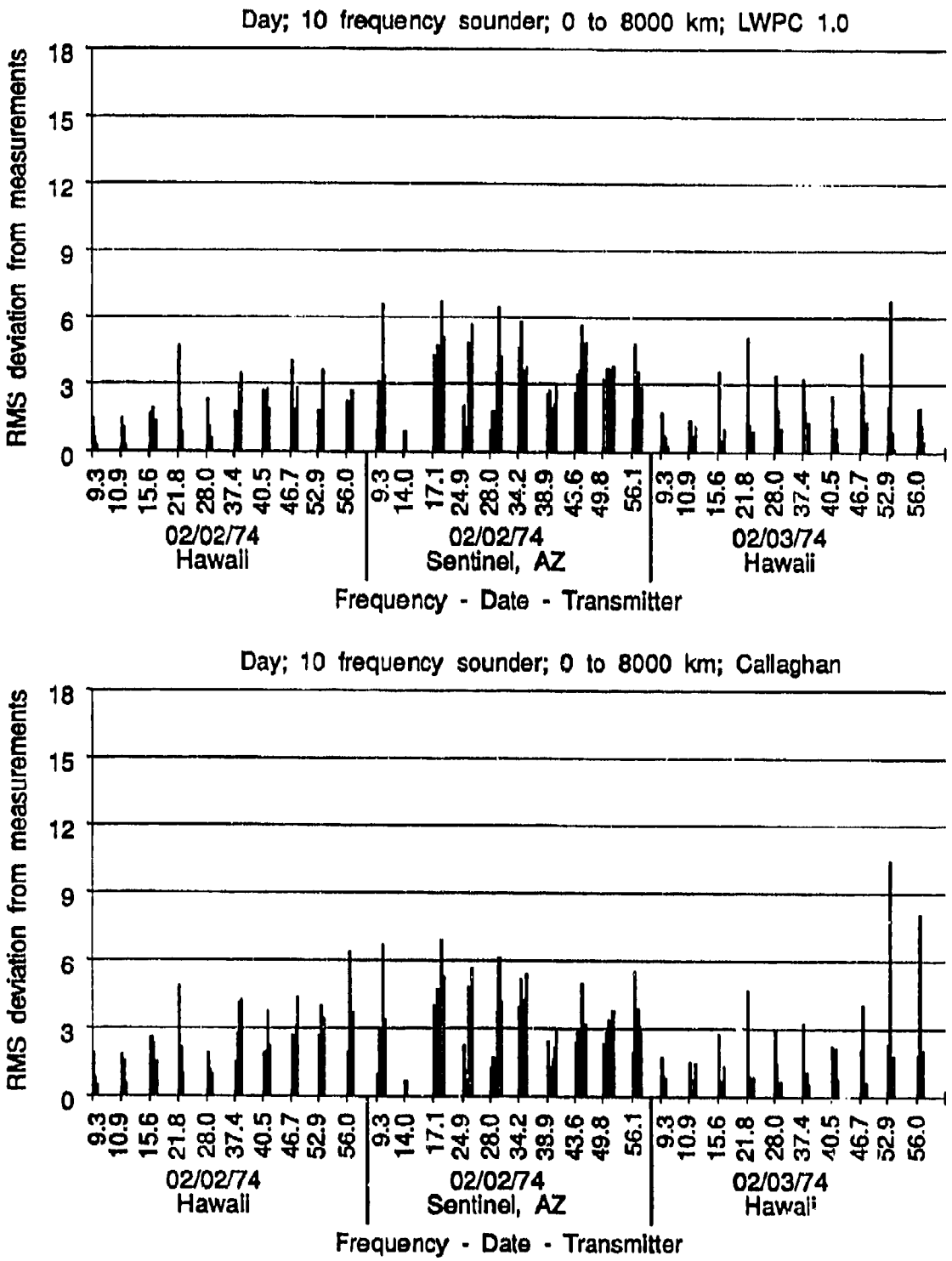

Figure 16. Comparison of models under daytime conditions using sounder data only.

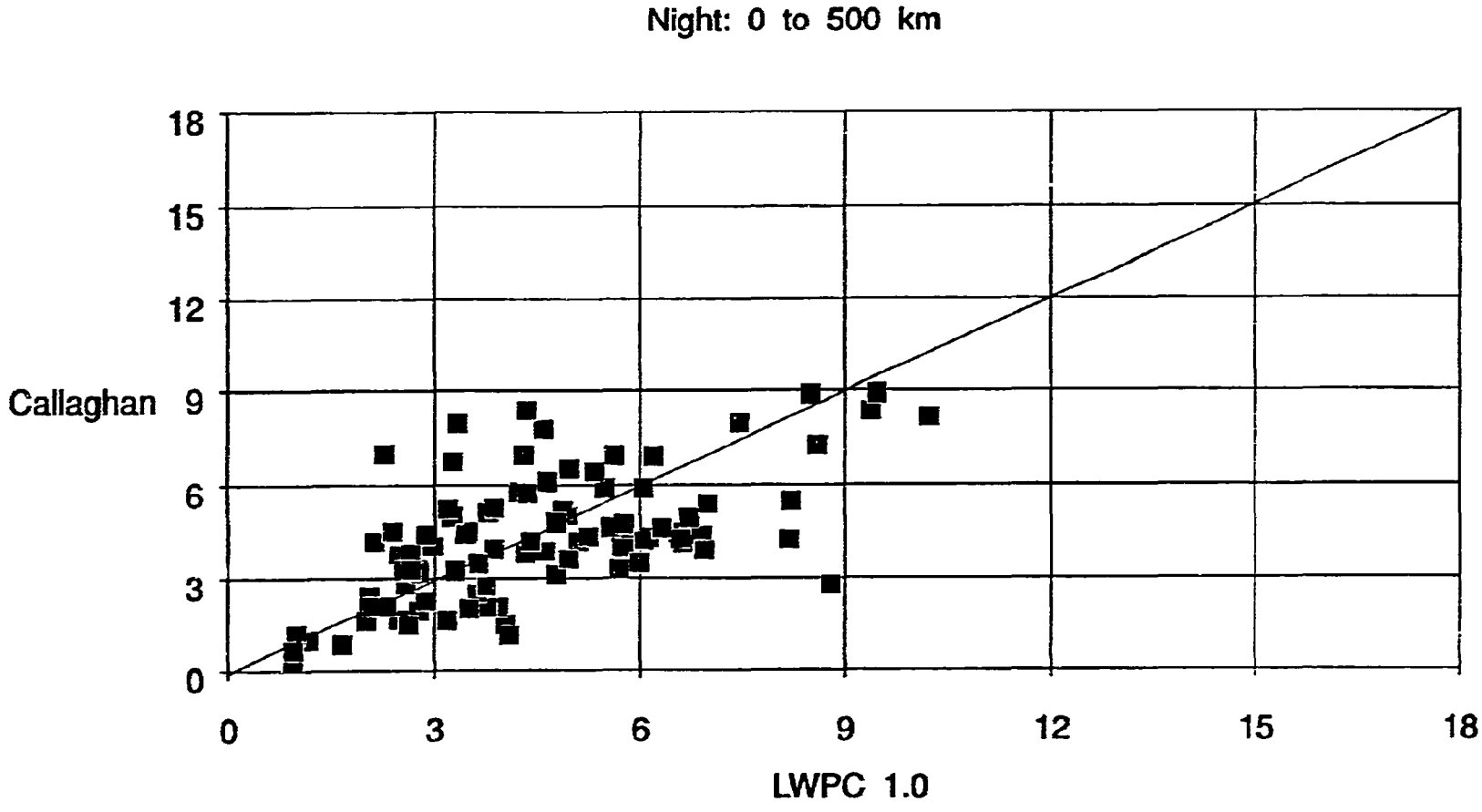

Figure 17. Scatter plot of the average absolute difference between the measurements and calculations using each ionospheric model over the distance range from 500 to 1000 km under nighttime conditions.

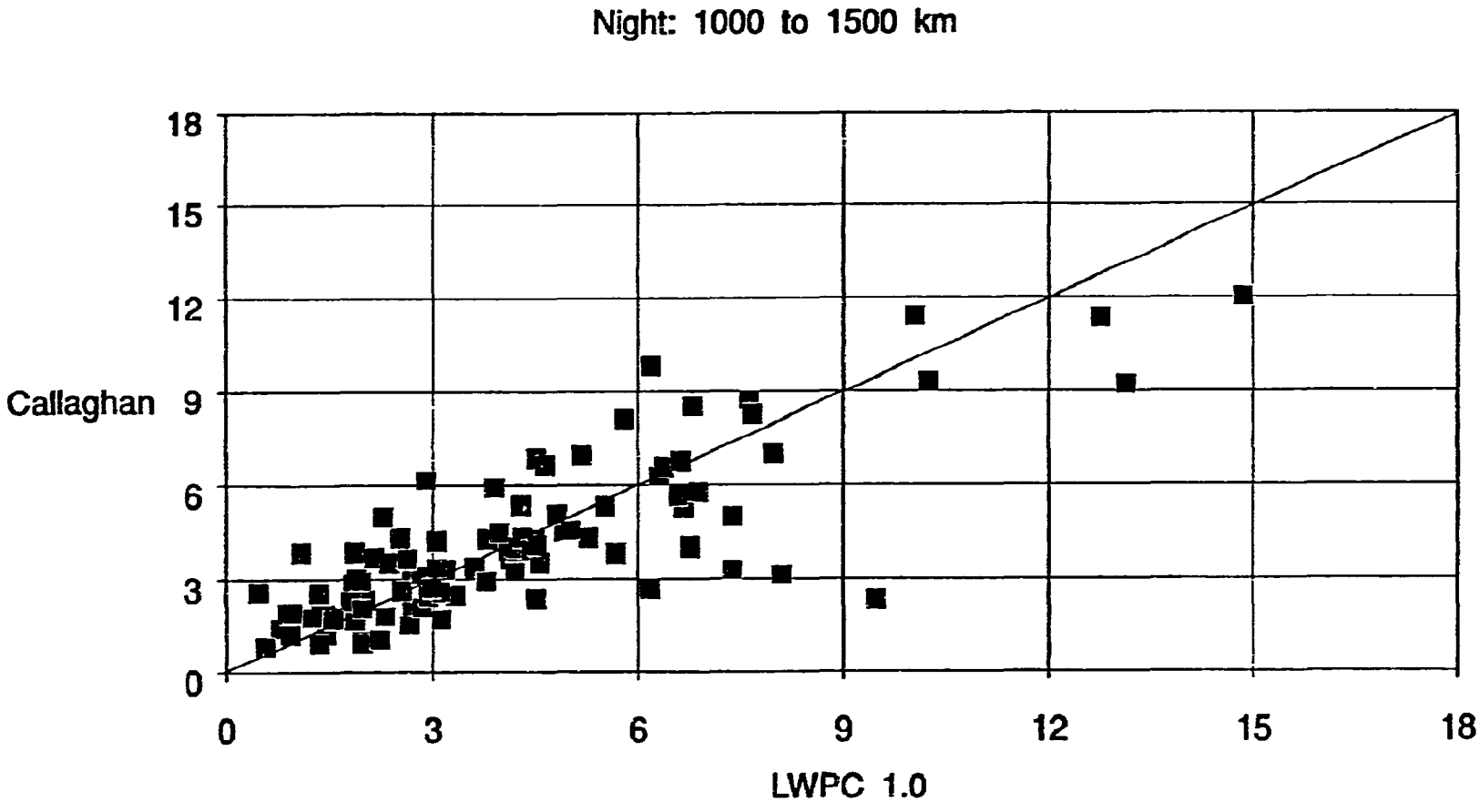

Figure 18. Scatter plots of the average absolute difference between the measurements and calculations using each ionospheric model over the distance range from 1000 to 1500 km under nighttime conditions.

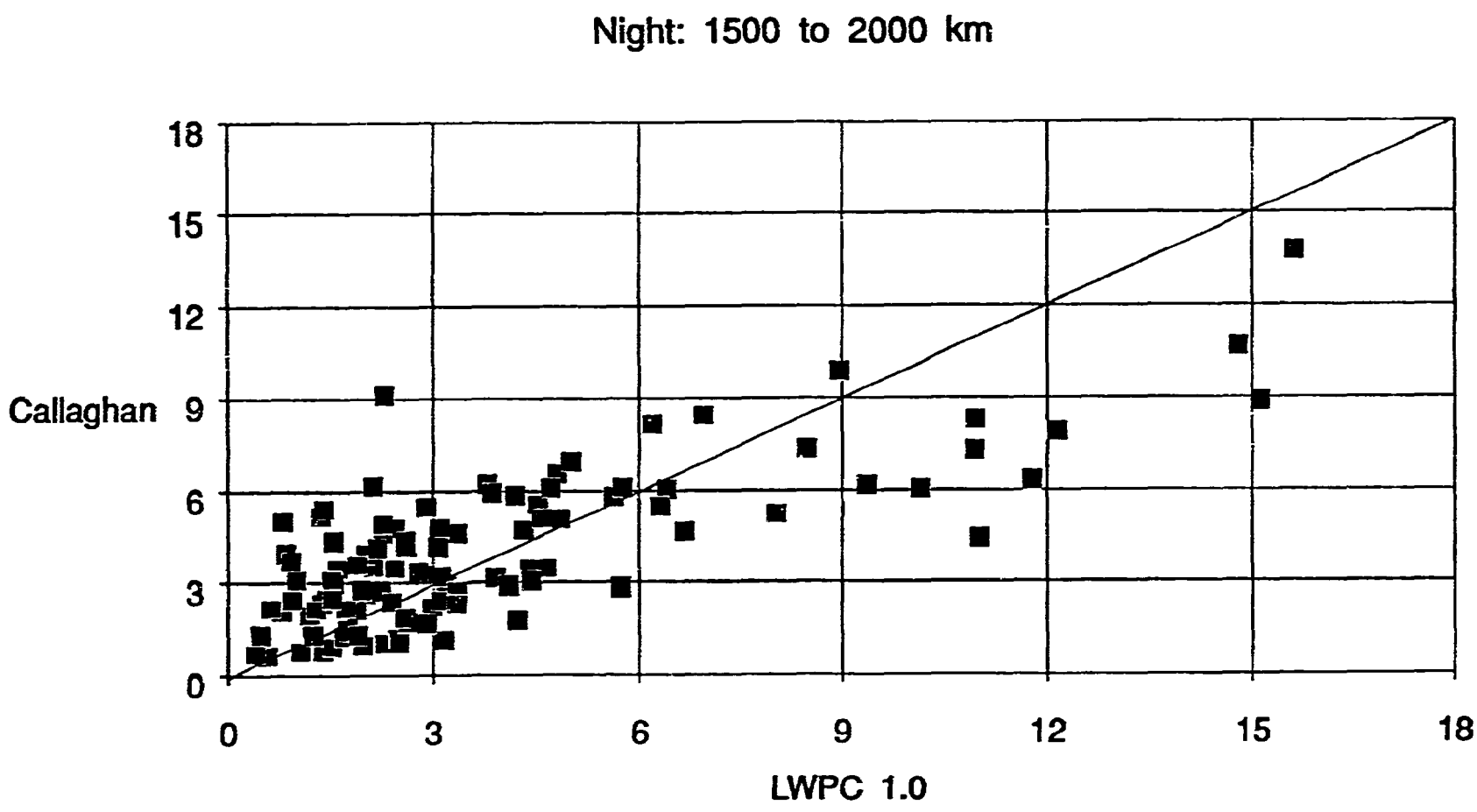

Figure 19. Scatter plot of the average absolute difference between the measurements and calculations using each ionospheric model over the distance range from 1500 to 2000 km under nighttime conditions.

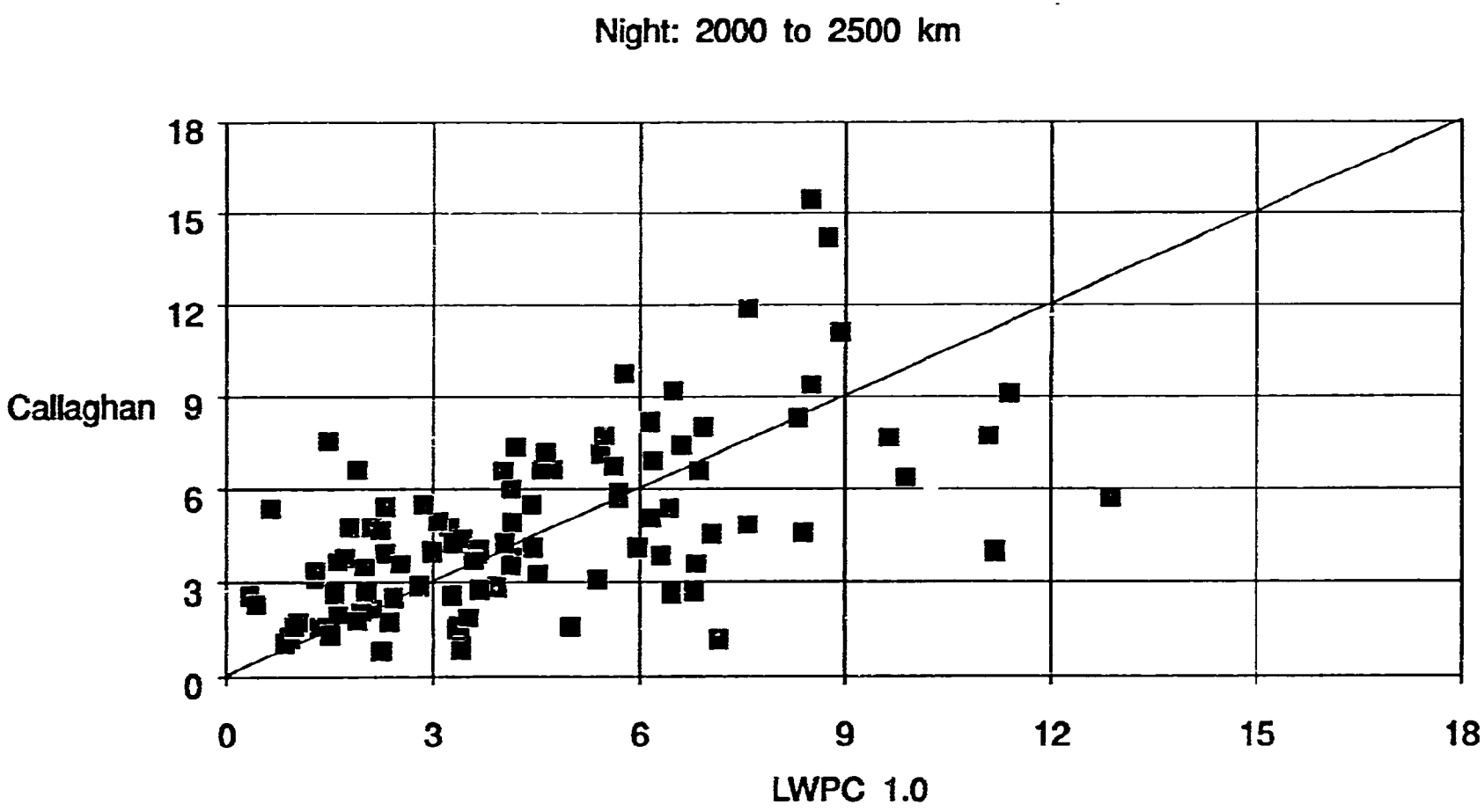

Figure 20. Scatter plot of the average absolute difference between the measurements and calculations using each ionospheric model over the distance range from 2000 to 2500 km under daytime conditions.

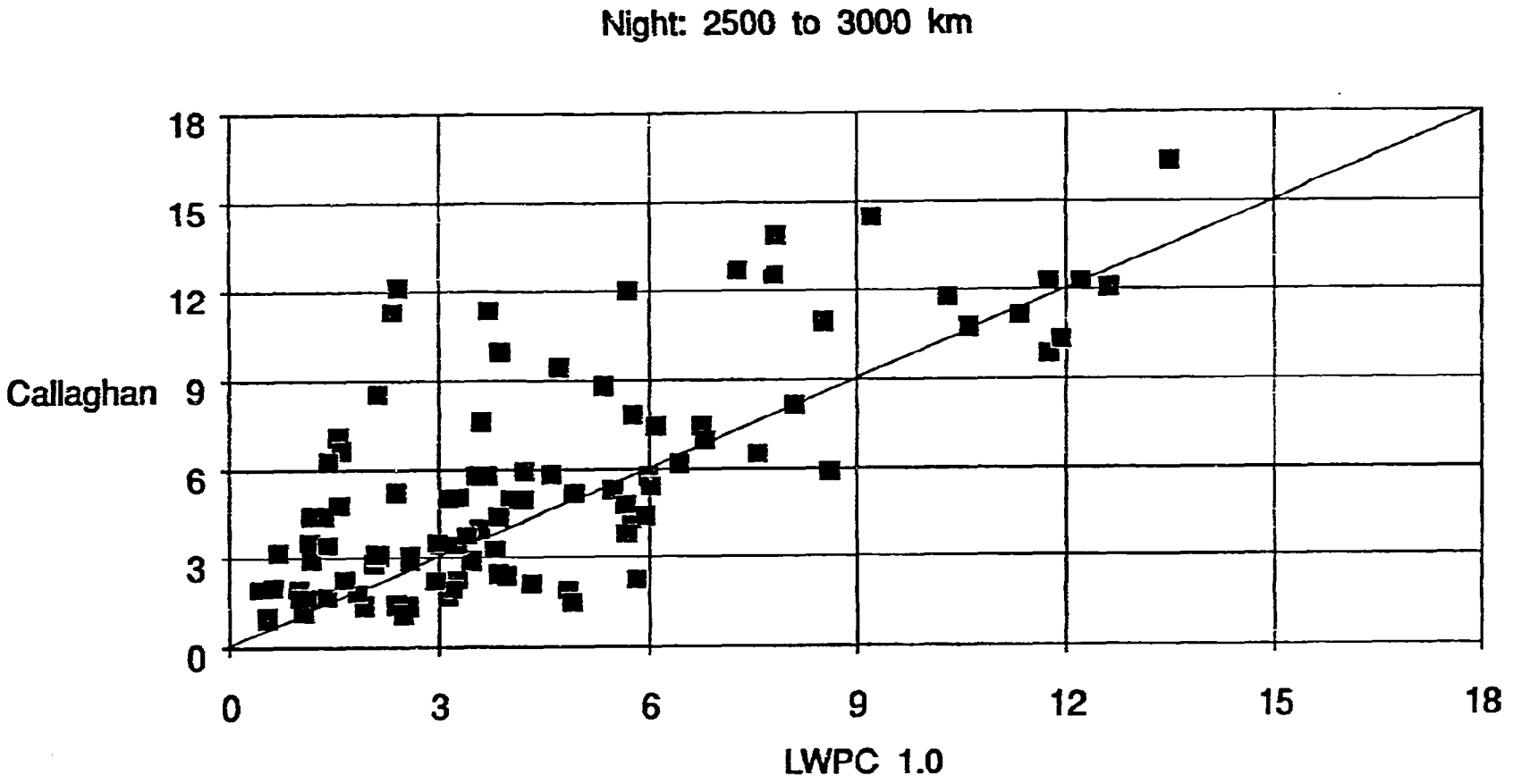

Figure 21. Scatter plot of the average absolute difference between the measurements and calculations using each ionospheric model over the distance range from 2500 to 3000 km under nighttime conditions.

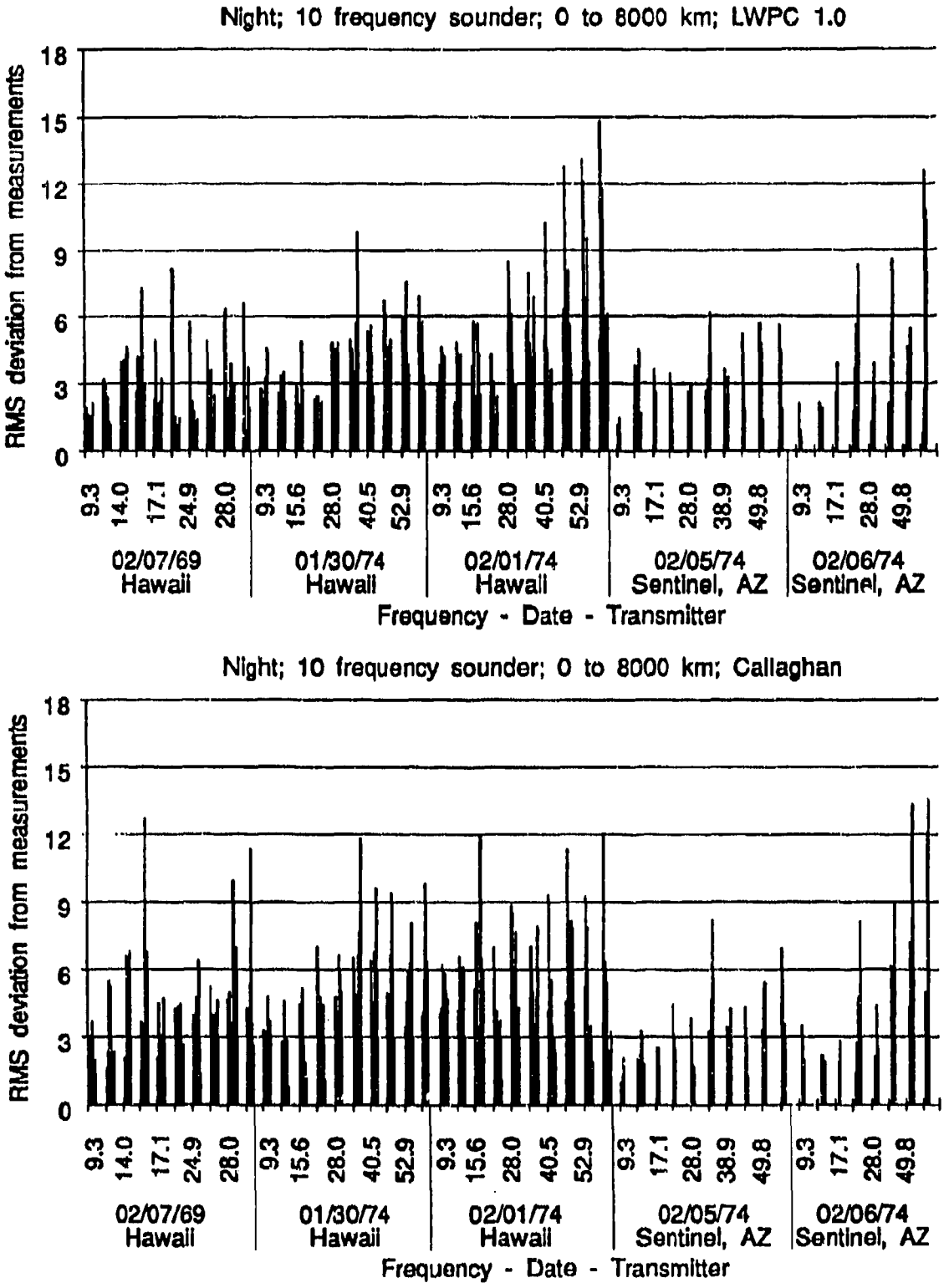

Figure 22. Comparison of models under nighttime conditions using sounder data only.

REFERENCES

Bickel, J. E., J. A. Ferguson and G. V. Stanley. 1970. "Experimental observation of magnetic field effects on VLF propagation at night," *Radio Science* 5, 19–25.

Ferguson, J. A. 1980. "Ionospheric Profiles for Predicting Nighttime VLF/LF Propagation," NOSC TR 530.

Ferguson, J. A., D. G. Morfitt and P. M. Hansen. 1985. "Statistical model for low-frequency propagation," *Radio Science* 20, 528–534.

Ferguson, J.A., and F.P. Snyder. 1987. "The Segmented Waveguide Program for Long Wavelength Propagation Calculations," NOSC TR 1071 (Apr).

Ferguson, J. A., and F. P. Snyder. 1989a. "Long-Wave Propagation Capability Program Description and User's Guide," NAVOCEANSYSCEN TD 1449, available from DTIC: ABD130808.

Ferguson, J. A., and F. P. Snyder. 1989b "The NAVOCEANSYSCEN's Long Wavelength Propagation Capability," NAVOCEANSYSCEN TD 1518, available from DTIC: ABD133690.

Ferguson, J. A. 1992. "A technique for determining operationally useful models of the ionospheric conductivity at very low frequencies," Submitted to Radio Science.

Gossard, E.E., Y.A. Gough, V.G. Noonkester, R.R. Pappert, I.J. Rothmuller, R.R. Smith and R. Winterbauer. 1966. "A Computer Program for VLF Model Constants in an Earth-Ionosphere Waveguide of Arbitrary Electron Density Distribution," DASA Interim Rpt. 671 (Sept).

Morfitt, D.G. 1977 "Effective Electron Density Distributions Describing VLF/LF Propagation Data," NOSC TR 141, (Sept).

Morfitt, D. G., J. A. Ferguson and F. P. Snyder. 1981. "Numerical Modeling of the Propagation Medium at ELF/VLF/LF," *AGARD Conference Proceedings Number 305*. September, Brussels, Belgium.

Morfitt, D.G., and C.H. Shellman. 1976. "'MODESRCH', An Improved Computer Program for Obtaining ELF/VLF/LF Mode Constants in an Earth-Ionosphere Waveguide," DNA Interim Rpt. 77T (Oct).

Pappert, R.A., and J.A. Ferguson. 1986. "VLF/LF Model Conversion Model Calculations for Air to Air Transmissions in the Earth-Ionosphere Waveguide," *Radio Science 21*, pp. 551–558.

Pappert, R.A., E.E. Gossard and I.J. Rothmuller. 1967. "A Numerical Investigation of Classical Approximations Used in VLF Propagation," *Radio Science 2*.

Pappert, R.A., L.R. Hitney. 1988. "Empirical modeling of nighttime easterly and westerly VLF propagation in the earth-ionosphere waveguide", *Radio Science 23*, pp. 599–611.

Pappert, R.A., W.F. Moler and L.R. Shockey. 1970. "A FORTRAN Program for Waveguide Propagation Which Allows for Both Vertical and Horizontal Dipole Excitation," DASA Interim Rpt. 702, (June).

Pappert, R.A., L.R. Shockey and W.F. Moler. 1971. "Results of a Numerical Mode Conversion Study at VLF," DNA Rpt. 2847P-2 (Dec).

Pappert, R.A., and L.R. Shockey. 1972. "Mode Conversion Program for an Inhomogeneous Anisotropic Ionosphere," DNA Interim Rpt. 722 (May).

Pappert, R.A., and L.R. Shockey. 1974. "A Simplified Mode Conversion Program for VLF Propagation in the Earth-Ionosphere Waveguide," DNA Interim Rpt. 751 (Oct).

Pappert, R.A., and R.R. Smith. 1971. "Numerical Results for VLF Mode Conversion in the Earth-Ionosphere Waveguide," DASA Interim Rpt. 712 (Apr).

Sheddy, C.H., Y.A. Gough and R.R. Pappert. 1968. "An Improved Computer Program for VLF Mode Constants in an Earth-Ionosphere Waveguide of Arbitrary Electron Density Distribution," DASA Interim Rpt. 682 (Jan).

Sheddy, C.H., R.A. Pappert, Y.A. Gough and W.F. Moler. 1968. "A FORTRAN Program for Mode Constants in an Earth-Ionosphere Waveguide," DASA Interim Rpt. 683 (May).

Shellman, C.H. 1986. "A New Version of MODESRCH Using Interpolated Values of the Magnetoionic Reflection Coefficients," NOSC TR 1143 (Aug).

Telecommunication Science Associates. 1991. "VLF/LF Data Analysis," NOSC TD 2082 (Mar).

APPENDIX A

Table A-1. Listing of the data used in the analysis.

Transmitter						Measurement						
Freq	Tlat		Tlong.		Bearing	Date	SSN	Rpt	Flg	D/N	β	h'
9.3	19.6	N	155.6	W	62.0	Feb 02, 1974	26	141	13	D	0.50	70.0
9.3	19.6	N	155.6	W	62.0	Feb 03, 1974	26	141	14	D	0.50	75.0
9.3	32.8	N	113.2	W	261.6	Feb 02, 1974	26	141	15	D		
10.2	66.4	N	13.1	E	292.0	Jul 01, 1970	112	141	42	D		
10.9	19.6	N	155.6	W	62.0	Feb 02, 1974	26	141	13	D	0.30	72.0
10.9	19.6	N	155.6	W	62.0	Feb 03, 1974	26	141	14	D	0.30	75.0
11.3	66.4	N	13.1	E	292.0	Jul 01, 1970	112	141	43	D		
13.6	66.4	N	13.1	E	297.4	Jul 01, 1970	112	141	44	D		
14.0	32.8	N	113.2	W	261.6	Feb 02, 1974	26	141	15	D	0.30	74.0
15.5	39.0	N	76.4	W	325.0	Jun 12, 1958	172	141	37	D		
15.6	19.6	N	155.6	W	62.0	Feb 02, 1974	26	141	13	D	0.30	72.0
15.6	19.6	N	155.6	W	62.0	Feb 03, 1974	26	141	14	D	0.30	75.0
16.6	21.4	N	158.1	W	271.7	Aug 01, 1955	41	141	12	D	0.50	70.0
16.6	21.4	N	158.1	W	63.8	Aug 01, 1955	41	141	12	D	0.50	70.0
17.1	32.8	N	113.2	W	261.6	Feb 02, 1974	26	141	15	D		
18.6	48.2	N	121.9	W	88.7	Jun 04, 1958	172	141	36	D	0.30	72.0
18.6	48.2	N	121.9	W	19.0	Jun 08, 1958	172	141	49	D	0.25	74.0
19.6	52.4	N	1.2	W	343.1	Jun 10, 1958	172	141	50	D	0.25	74.0
19.8	21.4	N	158.1	W	271.7	May 01, 1965	24	141	12	D	0.50	70.0
19.8	21.4	N	158.1	W	53.2	May 01, 1965	24	141	12	D	0.50	70.0
20.0	40.5	N	105.0	W	41.0	Sep 01, 1964	5	141	41	D	0.30	72.0
20.0	40.5	N	105.0	W	203.0	Sep 01, 1964	5	141	41	D	0.30	72.0
20.0	40.5	N	105.0	W	242.7	Sep 01, 1964	5	141	41	D	0.30	72.0
20.0	40.5	N	105.0	W	266.2	Sep 01, 1964	5	141	41	D		
20.0	40.5	N	105.0	W	98.3	Oct 01, 1964	20	141	41	D	0.30	72.0
20.0	40.5	N	105.0	W	77.0	Sep 01, 1965	17	141	41	D	0.30	72.0
20.0	40.5	N	105.0	W	117.5	Sep 01, 1965	17	141	41	D	0.30	72.0
20.0	40.5	N	105.0	W	154.6	Sep 01, 1965	17	141	41	D	0.30	72.0
20.0	40.5	N	105.0	W	305.2	Sep 01, 1965	17	141	41	D		
20.0	40.5	N	105.0	W	41.0	Jan 01, 1966	28	141	41	D		
20.0	40.5	N	105.0	W	154.6	Jan 01, 1966	28	141	41	D		
20.0	40.5	N	105.0	W	77.0	Feb 01, 1966	24	141	41	D	0.30	72.0
21.8	19.6	N	155.6	W	62.0	Feb 02, 1974	26	141	13	D	0.30	72.0
21.8	19.6	N	155.6	W	62.0	Feb 03, 1974	26	141	14	D	0.30	75.0
24.0	21.4	N	158.1	W	53.0	May 18, 1965	24	141	10	D	0.50	70.0
24.9	32.8	N	113.2	W	261.6	Feb 02, 1974	26	141	15	D	0.30	74.0
26.1	21.4	N	158.1	W	272.7	May 21, 1965	24	141	11	D		
26.1	21.4	N	158.1	W	257.9	May 22, 1965	24	141	11	D		
28.0	19.6	N	155.6	W	62.0	Feb 02, 1974	26	141	13	D	0.30	73.0
28.0	19.6	N	155.6	W	62.0	Feb 03, 1974	26	141	14	D	0.30	75.0
28.0	32.8	N	113.2	W	261.6	Feb 02, 1974	26	141	15	D	0.30	74.0

Table A-1. Listing of the data used in the analysis (continued).

Transmitter						Measurement						
Freq	Tlat		Tlong.		Bearing	Date	SSN	Rpt	Flg	D/N	β	h'
34.2	32.8	N	113.2	W	261.6	Feb 02, 1974	26	141	15	D		
37.4	19.6	N	155.6	W	62.0	Feb 02, 1974	26	141	13	D	0.35	73.0
37.4	19.6	N	155.6	W	62.0	Feb 03, 1974	26	141	14	D	0.30	75.0
38.9	32.8	N	113.2	W	261.6	Feb 02, 1974	26	141	15	D	0.30	74.0
40.5	19.6	N	155.6	W	62.0	Feb 02, 1974	26	141	13	D	0.35	73.0
40.5	19.6	N	155.6	W	62.0	Feb 03, 1974	26	141	14	D	0.30	75.0
43.6	32.8	N	113.2	W	261.6	Feb 02, 1974	26	141	15	D		
45.0	52.4	N	1.2	W	315.2	Jul 01, 1970	113	141	45	D		
46.7	19.6	N	155.6	W	62.0	Feb 02, 1974	26	141	13	D	0.35	73.0
46.7	19.6	N	155.6	W	62.0	Feb 03, 1974	26	141	14	D	0.30	75.0
49.8	32.8	N	113.2	W	261.6	Feb 02, 1974	26	141	15	D	0.30	75.0
52.9	19.6	N	155.6	W	62.0	Feb 02, 1974	26	141	13	D	0.35	73.0
52.9	19.6	N	155.6	W	62.0	Feb 03, 1974	26	141	14	D	0.30	75.0
56.0	19.6	N	155.6	W	62.0	Feb 02, 1974	26	141	13	D	0.35	73.0
56.0	19.6	N	155.6	W	62.0	Feb 03, 1974	26	141	14	D	0.30	75.0
56.1	32.8	N	113.2	W	261.6	Feb 02, 1974	26	141	15	D	0.30	75.0
60.0	40.5	N	105.0	W	41.0	Sep 01, 1964	5	141	40	D	0.30	72.0
60.0	40.5	N	105.0	W	203.0	Sep 01, 1964	5	141	40	D		
60.0	40.5	N	105.0	W	242.7	Sep 01, 1964	5	141	40	D		
60.0	40.5	N	105.0	W	266.2	Sep 01, 1964	5	141	40	D		
60.0	40.5	N	105.0	W	98.3	Oct 01, 1964	6	141	40	D	0.30	72.0
60.0	40.5	N	105.0	W	77.0	Sep 01, 1965	17	141	40	D	0.30	72.0
60.0	40.5	N	105.0	W	117.5	Sep 01, 1965	17	141	40	D	0.30	72.0
60.0	40.5	N	105.0	W	154.6	Sep 01, 1965	17	141	40	D	0.30	72.0
60.0	40.5	N	105.0	W	305.2	Sep 01, 1965	17	141	40	D		
60.0	40.5	N	105.0	W	154.6	Jan 01, 1966	28	141	40	D		
60.0	40.5	N	105.0	W	41.0	Jan 01, 1966	28	141	40	D		
60.0	40.5	N	105.0	W	77.0	Feb 01, 1966	24	141	40	D		
60.0	52.4	N	1.2	W	317.0	Jul 01, 1970	113	141	47	D	0.30	72.0
9.3	19.6	N	155.6	W	59.0	Feb 07, 1969	121	141	22	N	0.35	87.0
9.3	19.6	N	155.6	W	62.0	Jan 30, 1974	26	141	23	N	0.30	87.0
9.3	19.6	N	155.6	W	62.0	Feb 01, 1974	26	141	24	N	0.30	89.0
9.3	32.8	N	113.2	W	12.6	Feb 05, 1974	26	530	14	N		
9.3	32.8	N	113.2	W	12.6	Feb 06, 1974	26	530	14	N		
10.2	21.4	N	157.8	W	200.6	Jan 29, 1969	104	141	18	N		
10.2	21.4	N	157.8	W	272.7	Feb 03, 1969	121	141	19	N	0.50	87.0
10.2	21.4	N	157.8	W	61.7	Feb 07, 1969	121	141	20	N	0.40	87.0
10.9	19.6	N	155.6	W	59.0	Feb 07, 1969	121	141	22	N	0.40	87.0
10.9	19.6	N	155.6	W	62.0	Jan 30, 1974	26	141	23	N	0.40	86.0
10.9	19.6	N	155.6	W	62.0	Feb 01, 1974	26	141	24	N	0.30	89.0
13.6	21.4	N	157.8	W	200.6	Jan 29, 1969	104	141	18	N		

Table A-1. Listing of the data used in the analysis (continued).

Transmitter						Measurement						
Freq	Tlat		Tlong.		Bearing	Date	SSN	Rpt	Fig	D/N	β	h'
13.6	21.4	N	157.8	W	80.1	Feb 03, 1969	121	141	19	N	0.50	87.0
13.6	21.4	N	157.8	W	61.7	Feb 07, 1969	121	141	20	N	0.50	87.0
14.0	19.6	N	155.6	W	59.0	Feb 07, 1969	121	141	22	N	0.50	87.0
14.0	32.8	N	113.2	W	12.6	Feb 05, 1974	26	530	14	N		
14.0	32.8	N	113.2	W	12.6	Feb 06, 1974	26	530	14	N		
15.5	39.0	N	76.4	W	301.0	Nov 16, 1957	201	530	2	N	0.60	77.0
15.5	39.0	N	76.4	W	01.0	Dec 16, 1957	200	530	2	N	0.60	76.0
15.6	19.6	N	155.6	W	59.0	Feb 07, 1969	121	141	22	N	0.50	87.0
15.6	19.6	N	155.6	W	62.0	Jan 30, 1974	26	141	23	N	0.50	86.0
15.6	19.6	N	155.6	W	62.0	Feb 01, 1974	26	141	24	N	0.40	88.0
16.0	52.4	N	1.2	W	287.1	Oct 05, 1975	14	530	21	N		
16.0	52.4	N	1.2	W	287.1	Oct 05, 1975	14	530	10	N		
16.0	52.4	N	1.2	W	12.2	Jan 09, 1977	17	530	12	N		
16.0	52.4	N	1.2	W	12.2	Jan 10, 1977	17	530	12	N		
16.0	52.4	N	1.2	W	21.2	Feb 04, 1977	18	530	12	N		
16.0	52.4	N	1.2	W	21.2	Feb 04, 1977	18	530	22	N		
16.0	52.4	N	1.2	W	21.2	Feb 06, 1977	18	530	12	N		
16.0	52.4	N	1.2	W	21.2	Feb 06, 1977	18	530	22	N		
16.4	66.4	N	13.1	E	283.7	Jan 06, 1977	17	530	11	N	0.40	80.0
16.4	66.4	N	13.1	E	283.7	Feb 02, 1977	18	530	11	N	0.40	76.0
16.4	66.4	N	13.1	E	352.0	Feb 06, 1977	18	530	13	N		
17.1	19.6	N	155.6	W	59.0	Feb 07, 1969	121	141	22	N	0.50	87.0
17.1	32.8	N	113.2	W	12.6	Feb 05, 1974	26	530	14	N		
17.1	32.8	N	113.2	W	12.6	Feb 06, 1974	26	530	14	N		
17.8	44.6	N	67.3	W	55.1	May 18, 1975	17	530	8	N	0.40	85.0
17.8	44.6	N	67.3	W	55.1	May 18, 1975	17	530	19	N		
17.8	44.6	N	67.3	W	55.1	May 21, 1975	17	530	19	N	0.40	85.0
17.8	44.6	N	67.3	W	55.1	May 21, 1975	17	530	8	N		
17.8	44.6	N	67.3	W	55.1	Oct 03, 1975	14	530	19	N		
17.8	44.6	N	67.3	W	55.1	Oct 03, 1975	14	530	8	N		
17.8	44.6	N	67.3	W	55.1	Oct 05, 1975	14	530	8	N	0.50	87.0
17.8	44.6	N	67.3	W	55.1	Oct 05, 1975	14	530	19	N		
17.8	44.6	N	67.3	W	33.1	Dec 01, 1976	15	530	20	N		
17.8	44.6	N	67.3	W	33.1	Dec 01, 1976	15	530	9	N	0.30	87.0
17.8	44.6	N	67.3	W	286.2	Dec 06, 1976	15	530	16	N		
17.8	44.6	N	67.3	W	286.2	Dec 06, 1976	15	530	4	N	0.40	88.0
17.8	44.6	N	67.3	W	295.5	Dec 07, 1976	15	530	4	N	0.40	88.0
17.8	44.6	N	67.3	W	295.5	Dec 07, 1976	15	530	16	N		
17.8	44.6	N	67.3	W	55.1	Jan 06, 1977	17	530	20	N		
17.8	44.6	N	67.3	W	55.1	Jan 06, 1977	17	530	9	N	0.30	84.0
17.8	44.6	N	67.3	W	286.2	Jan 12, 1977	17	530	4	N	0.40	87.0
17.8	44.6	N	67.3	W	295.5	Jan 14, 1977	18	530	16	N	0.40	82.0
17.8	44.6	N	67.3	W	295.5	Jan 14, 1977	18	530	4	N	0.40	82.0

Table A-1. Listing of the data used in the analysis (continued).

Transmitter						Measurement						
Freq	Tlat		Tlong.		Bearing	Date	SSN	Rpt	Fig	D/N	β	h'
17.8	44.6	N	67.3	W	33.1	Feb 02, 1977	18	530	20	N		
17.8	44.6	N	67.3	W	33.1	Feb 02, 1977	18	530	9	N	0.30	84.0
17.8	44.6	N	67.3	W	286.2	Feb 10, 1977	18	530	4	N	0.40	87.0
17.8	44.6	N	67.3	W	286.2	Feb 10, 1977	18	530	16	N	0.40	87.0
17.8	44.6	N	67.3	W	295.5	Feb 11, 1977	18	530	16	N	0.40	80.0
17.8	44.6	N	67.3	W	295.5	Feb 11, 1977	18	530	4	N	0.40	80.0
18.6	48.2	N	121.9	W	88.7	Nov 16, 1957	201	530	3	N	0.60	77.0
18.6	48.2	N	121.9	W	88.7	Dec 16, 1957	200	530	3	N	0.60	76.0
18.6	48.2	N	121.9	W	88.7	Jan 24, 1969	104	530	3	N	0.60	82.0
18.6	48.2	N	121.9	W	88.7	Jan 26, 1969	104	530	3	N	0.60	76.0
18.6	48.2	N	121.9	W	240.1	Jan 27, 1969	104	530	5	N	0.60	82.0
18.6	48.2	N	121.9	W	240.1	Jan 12, 1977	17	530	17	N		
18.6	48.2	N	121.9	W	240.1	Jan 12, 1977	17	530	5	N	0.60	87.0
18.6	48.2	N	121.9	W	74.5	Jan 14, 1977	18	530	15	N		
18.6	48.2	N	121.9	W	74.5	Jan 14, 1977	18	530	3	N	0.40	82.0
18.6	48.2	N	121.9	W	240.1	Feb 10, 1977	18	530	17	N		
18.6	48.2	N	121.9	W	240.1	Feb 10, 1977	18	530	5	N	0.60	87.0
18.6	48.2	N	121.9	W	74.5	Feb 11, 1977	18	530	15	N		
18.6	48.2	N	121.9	W	74.5	Feb 11, 1977	18	530	3	N	0.40	80.0
21.4	39.0	N	76.4	W	301.0	Jan 24, 1969	104	530	2	N	0.60	82.0
21.4	39.0	N	76.4	W	301.0	Jan 26, 1969	104	530	2	N	0.60	76.0
21.8	19.6	N	155.6	W	59.0	Feb 07, 1969	121	141	22	N	0.50	88.0
21.8	19.6	N	155.6	W	62.0	Jan 30, 1974	28	141	23	N	0.70	87.0
21.8	19.6	N	155.6	W	62.0	Feb 01, 1974	26	141	24	N	0.50	88.0
23.4	21.4	N	158.1	W	38.4	Jan 27, 1969	104	530	6	N		
23.4	21.4	N	158.1	W	200.1	Jan 29, 1969	104	141	17	N	0.50	85.5
23.4	21.4	N	158.1	W	200.1	Jan 31, 1969	104	141	17	N	0.50	85.5
23.4	21.4	N	158.1	W	272.7	Feb 02, 1969	121	141	17	N		
23.4	21.4	N	158.1	W	272.7	Feb 03, 1969	121	141	17	N		
23.4	21.4	N	158.1	W	61.8	Feb 07, 1969	121	141	17	N		
23.4	21.4	N	158.1	W	38.4	Dec 06, 1976	15	530	6	N	0.40	89.0
23.4	21.4	N	158.1	W	3.5	Jan 11, 1977	17	530	7	N		
23.4	21.4	N	158.1	W	3.5	Jan 11, 1977	17	530	18	N	0.60	87.0
24.9	19.6	N	155.6	W	59.0	Feb 07, 1969	121	141	22	N	0.50	88.0
24.9	32.8	N	113.2	W	12.6	Feb 05, 1974	26	530	14	N		
26.5	19.6	N	155.6	W	59.0	Feb 07, 1969	121	141	22	N	0.50	88.0
28.0	19.6	N	155.6	W	59.0	Feb 07, 1969	121	141	22	N	0.50	88.0
28.0	19.6	N	155.6	W	62.0	Jan 30, 1974	28	141	23	N	1.00	88.0
28.0	19.6	N	155.6	W	62.0	Feb 01, 1974	26	141	24	N	0.50	89.0
28.0	32.8	N	113.2	W	12.6	Feb 05, 1974	26	530	14	N		
31.1	19.6	N	155.6	W	59.0	Feb 07, 1969	121	141	22	N	0.60	88.0
34.2	32.8	N	113.2	W	12.6	Feb 05, 1974	26	530	14	N		

Table A-1. Listing of the data used in the analysis (continued).

Transmitter						Measurement						
Freq	Tlat		Tlong.		Bearing	Date	SSN	Rpt	Fig	D/N	β	h'
37.4	19.6	N	155.6	W	62.0	Jan 30, 1974	28	141	23	N	1.20	88.0
37.4	19.6	N	155.6	W	62.0	Feb 01, 1974	26	141	24	N	0.60	88.0
38.9	32.8	N	113.2	W	12.6	Feb 05, 1974	26	530	14	N		
40.5	19.6	N	155.6	W	62.0	Jan 30, 1974	28	141	23	N	1.20	88.0
40.5	19.6	N	155.6	W	62.0	Feb 01, 1974	26	141	24	N	0.60	88.0
43.4	32.8	N	113.2	W	12.6	Feb 05, 1974	26	530	14	N		
43.4	32.8	N	113.2	W	12.6	Feb 06, 1974	26	530	14	N		
46.7	19.6	N	155.6	W	62.0	Jan 30, 1974	28	141	23	N	1.20	88.0
46.7	19.6	N	155.6	W	62.0	Feb 01, 1974	26	141	24	N	0.70	88.0
49.8	32.8	N	113.2	W	12.6	Feb 05, 1974	26	530	14	N		
52.9	19.6	N	155.6	W	62.0	Jan 30, 1974	28	141	23	N	1.20	88.0
52.9	19.6	N	155.6	W	62.0	Feb 01, 1974	26	141	24	N	0.70	88.0
56.0	19.6	N	155.6	W	62.0	Jan 30, 1974	28	141	23	N	1.20	88.0
56.0	19.6	N	155.6	W	62.0	Feb 01, 1974	26	141	24	N	0.70	88.0
56.1	32.8	N	113.2	W	12.6	Feb 05, 1974	26	530	14	N		

NOTES: SSN = Zurich smoothed sunspot number for the measurement month.
D/N = Day/Night
TLAT = Transmitter latitude
TLong = Transmitter Longitude

REPORT DOCUMENTATION PAGE

Form Approved
OMB No. 0704-0188

1. AGENCY USE ONLY (Leave blank)	2. REPORT DATE	3. REPORT TYPE AND DATES COVERED
	November 1992	Final: November 1992

4. TITLE AND SUBTITLE

A REVIEW OF THE IONOSPHERIC MODEL FOR THE LONG WAVE PREDICTION CAPABILITY

5. FUNDING NUMBERS

PN: X1083
PE: 0101402N
AN: DN587543

6. AUTHOR(S)

J. A. Ferguson

7. PERFORMING ORGANIZATION NAME(S) AND ADDRESS(ES)

Naval Command, Control and Ocean Surveillance Center
RDT&E Division
San Diego, CA 92152-5001

8. PERFORMING ORGANIZATION REPORT NUMBER

TD 2393

9. SPONSORING/MONITORING AGENCY NAME(S) AND ADDRESS(ES)

Space and Naval Warfare Systems Command
PMW 152-23
Washington DC 20363-5100

10. SPONSORING/MONITORING AGENCY REPORT NUMBER

11. SUPPLEMENTARY NOTES

12a. DISTRIBUTION/AVAILABILITY STATEMENT

Approved for public release; distribution is unlimited.

12b. DISTRIBUTION CODE

Bu Prog Development/Evaluation

13. ABSTRACT (Maximum 200 words)

The Naval Command, Control and Ocean Surveillance Center's Long Wave Prediction Capability (LWPC) has a built-in ionospheric model. The latter was defined after a review of the literature comparing measurements with calculations. Subsequent to this original specification of the ionospheric model in the LWPC, a new collection of data were obtained and analyzed. The new data were collected aboard a merchant ship named the *Callaghan* during a series of trans-Atlantic trips over a period of a year. This report presents a detailed analysis of the ionospheric model currently in use by the LWPC and the new model suggested by the shipboard measurements. We conclude that, although the fits to measurements are almost the same between the two models examined, the current LWPC model should be used because it is better than the new model for nighttime conditions at long ranges. This conclusion supports the primary use of the LWPC model for coverage assessment that requires a valid model at the limits of a transmitter's reception.

14. SUBJECT TERMS

communications
high voltage
measurement
very low frequency & low frequency antennas

15. NUMBER OF PAGES

46

16. PRICE CODE

17. SECURITY CLASSIFICATION OF REPORT	18. SECURITY CLASSIFICATION OF THIS PAGE	19. SECURITY CLASSIFICATION OF ABSTRACT	20. LIMITATION OF ABSTRACT
UNCLASSIFIED	UNCLASSIFIED	UNCLASSIFIED	SAME AS REPORT

21a. NAME OF RESPONSIBLE INDIVIDUAL	21b. TELEPHONE *(Include Area Code)*	21c. OFFICE SYMBOL
J. A. Ferguson	(619) 553–3062	Code 542

INITIAL DISTRIBUTION

Code 0012	Patent Counsel	(1)
Code 144	V. Ware	(1)
Code 50	H. O. Porter	(1)
Code 54	J. H. Richter	(1)
Code 542	J. A. Ferguson	(30)
Code 961	Archive/Stock	(6)
Code 964B	Library	(2)

Defense Technical Information Center
Alexandria, VA 22304-6145 (4)

NCCOSC Washington Liaison Office
Washington, DC 20363-5100

Center for Naval Analyses
Alexandria, VA 22302-0268

Navy Acquisition, Research & Development
Information Center (NARDIC)
Washington, DC 20360-5000

GIDEP Operations Center
Corona, CA 91718-8000